A String Theory for 3-Manifolds with a Kleinian Action

Sóstenes Lins (sostenes@dmat.ufpe.br)
Departamento de Matemática da UFPE
50739 Recife Brasil

October 21, 2001

Contents

Abstract

In this paper [1] we show that a class of orientable 3-manifolds can arise as (and be presented by) the *"interaction of charged strings"*. The presentation is very concise and it encodes complete information for producing the manifold as the union of closed balls, by providing instructions on how to identify the boundaries of these balls.

The central issue of considering this class of manifolds is that (often) the string presentation is capable of revealing the structure of the manifolds in the sense of displaying ways to form them as the *"interaction of smaller"* closed manifolds in the class.

We also prove some Theorems on the recognition of sufficiently large 3-manifolds. The essential torus, which characterizes such manifolds arises simply as an special pair of *"segments"* (which are special connected substrings). Cutting along such torus, is internal to the the string presentation and it suggests a natural way to close the boundary of the resulting manifold.

Finally, we use the string presentation theory to display a complete catalogue of closed orientable 3-manifolds whose fundamental groups are not cyclic nor free products and which have *"gem-complexity"* at most 13.

---

1   Basic Terminology, Examples and an Overview of the Results

1.1   Introduction

A very appealing and seductive aspect of the subject of 3-manifolds is the tremendous richness of forms in which they manifest themselves. Of these forms, one of the most elegant and successful is Kirby's presentation as framed links [Kir78] based in the fundamental result on constructing 3-manifolds by surgery due to Wallace [Wal60] and Lickorish [Lic62]. The objects which we use here to present 3-manifolds, *gists* or *string presentations* are, on the apparence, similar to framed links. However they do not encode surgery descriptions, but obtain the manifold directly by inducing a cell decomposition for it as closed *i*-balls, $i = 0, 1, 2, 3$. Here is such an object, presenting the original *homology sphere of Poincaré*, the manifold whose fundamental group is the binary dodecahedral group, P_{120}:
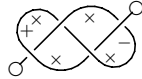
The string presentation comes from an encoding of the symmetries of a 3-*gem* or 3-*dimensional graph encoded manifold*, (see next section) which yields a manifold as the union of closed balls with a recipe to identify their boundary. In the specific case above, Poincaré sphere arises from the following four balls whose boundaries are identified so as to match equally labeled vertices:
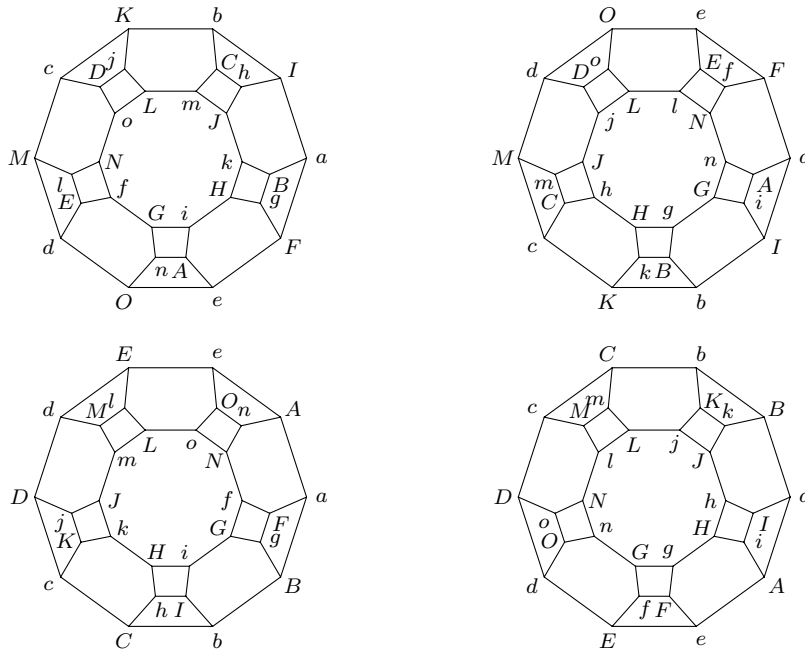
The four balls (including the respective labellings) are uniquely recoverable from the above given string presentation.

Being a new language we want to start by giving various examples. We choose various well known manifolds and present them as *"interacting charged strings"*. This is partially done in the next subsection; it is continued in the final section, which is a complete catalogue of closed orientable 3-manifolds whose fundamental groups are not cyclic, not free products and which have a "complexity" up to a certain size.

In subsection 1.3 we show how the simplest example of the an important infinite sequence of 3-manifolds given by Boileau and Zieschang [BZ84], becomes even more simple, because it admits a small string presentation. We use a Heegaard diagram due to Montesinos [Mon89], and the simplification algorithm developed in [LD91] to get the string presentation.

In subsection 1.4 we display a string presentation for the smallest (in terms of volume) known hyperbolic 3-manifold, W^3. At first we noted ([LS94]) an isomorphism of the fundamental group of the 3-manifold induced by an specific 3-gem, $\mathcal{S}(3, 7, 4, 1)$, and the one of W^3. In fact the presentation for $\pi_1(W^3)$ was due to J. Weeks, who also provided a surgery presentation for W^3 (personal communication). From this presentation, we get a proof that the manifolds are homeomorphic. This proof appears in [Lin95]. The string presentation for W^3 follows from a simplification of $\mathcal{S}(3, 7, 4, 1)$.

In subsection 1.5 we introduce the definitions so as to permit in subsectio 1.6 the statements of the main results of the paper. They are sufficient conditions for the detection, in a string presentation, of embedded non-separating

tori, which characterize sufficiently large 3-manifolds and a decomposition Theorem into closed 3-manifolds induced by separating tori.

The essential tori which we detect, can be (in 4 out of 5 cases) splitted internally in the theory. In all the cases, however, the theory suggests an entirely natural way to close the resulting boundary. We believe that there are connections to be found between the string theory and the decomposition theory of Jaco and Shalen [JS79] and Jorhannsen [Jor79].

In section 2 we present the primitive and generating connection with the theory of 3-gems providing complete examples.

In section 3 we prove many basic results of the theory starting with the one that shows that however there are 3-manifolds without string presentations, four disjoint copies of any manifold M^3 has such presentation. And so does the quintuple connected sum

$$M^3 \# M^3 \# M^3 \# M^3 \# \mathbf{RP}^3.$$

The rest of the basic results are on small local changes in the string presentations and their connections with Dehn-Lickorish and even Dehn-Lickorish surgeries.

In section 4 we treat the recognition of embedded spheres and tori and the decomposition Theorems.

The final section 5 is a catalogue for all the closed orientable prime 3-manifolds which are not non-lens spaces and which have *gem-complexities* (see next section and the last one) at most 13.

Many basic questions are not yet answered. The fundamental ones are the following:

- *What is*, topologically, the class $\mathcal{G}$ of 3-manifolds which admit a string presentation? [2]

- Is there an an easy general way to get a framed link presentation from a string presentation?[3]

- Are there simple moves connecting by a finite sequence any two string presentations? Any two presenting the same manifold?

1.2 Simple Examples

To give a general feeling of 3-manifolds as charged strings interacting we start by giving some examples.

The gists below induce closed 3-balls and a recipe to identify their boundaries producing the 3-sphere $\mathbf{S}^3$, the 3-projective space $\mathbf{RP}^3$, $\mathbf{S}^2 \times \mathbf{S}^1$, the 3-torus $\mathbf{S}^1 \times \mathbf{S}^1 \times \mathbf{S}^1 = \mathbf{T}^3$ and the quaternionic space $\mathbf{S}^3/Q^8$. The last gist already exibits most of the elements of the string presentation, which we shall define in the next subsection: open and closed strings, $\div$crossings and charges of all three types; a $\times$crossing is present in the gist for the 3-torus.

The presentation is by no means unique in any sense. Here are some more small gists presenting the same manifolds:

The above pairs of gists for the projective 3-space and the 3-torus induce exactly the same cell decomposition of these manifolds. Below we present still another (the third) gist for the the same cell decomposition of $\mathbf{RP}^3$ and two infinite families of lens spaces:


---

[2]Four disjoint copies of any 3-manifold is in this class $\mathcal{G}$.

[3]There is a subtle connection with the framed linked presentation; it seems to work for 2-folded branched coverings of S^3. However, how exactly needs to be better mastered.

Here are string presentations for the binary tetrahedral space, $\mathbf{S}^3/P_{24}$, the binary octhedral space, $\mathbf{S}^3/P_{48}$, and the original *Poincaré's homology sphere*, the binary dodecahedral space $\mathbf{S}^3/P_{120}$. These are not the smallest ones, but show them as a sequence, closely related with the lens spaces $\mathbf{L}_{6,1}$, $\mathbf{L}_{7,1}$ and $\mathbf{L}_{8,1}$:

Indeed there are global simple conditions on the local configurations below (which are met by the above 3 gists) so that hold (see section 3):
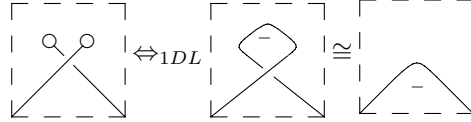
The symbol $\cong$ means that there is a homeomorphism between the presented spaces. The subscript $_{1DL}$ of the equivalence means that the spaces are connected by performing a single Dehn-Lickorish surgery. By replacing the double end by a minus charge in the three manifolds above, we get, respectively, the lens spaces $\mathbf{L}_{6,1}$, $\mathbf{L}_{7,1}$ and $\mathbf{L}_{8,1}$.

Compare the above interaction of strings producing $\mathbf{S}^3/P_{120}$ with the following surgery instructions to get the same manifold, see pag 310 of [Rol76]:

There is more than a coincidence here. The deep connection between the theories are not yet fully understood.

Let $\mathbf{T}_n^2$ denote the closed orientable surface of genus n. A family for the 3-manifolds $\mathbf{S}^1 \times \mathbf{T}_n^2$ starts with:

In general, to get a string presentation for $\mathbf{S}^1 \times \mathbf{T}_{n+1}^2$, just introduce an internal closed string in the one for $\mathbf{S}^1 \times \mathbf{T}_n^2$ with an alternating pattern of underpasses and overpasses and conclude by putting a minus charge on the top and on the bottom points of the new string, as indicated. This family of presentations together with the theory to be developed in section 3 provide a proof of the following fact, which accounts for an interesting kind of distributivity:

Proposition 1 *There is an embedded solid torus V_1 in $\mathbf{S}^1 \times \mathbf{T}_n^2$ and another one, V_2, in the connected sum of $2n$ copies of $\mathbf{S}^2 \times \mathbf{S}^1$ so that*

$$\mathbf{S}^1 \times \mathbf{T}_n^2 \backslash V_1 \cong \#_{2n} \left(\mathbf{S}^2 \times \mathbf{S}^1 \right) \backslash V_2.$$

Indeed,

$$\mathbf{S}^1 \times \underbrace{\left((\mathbf{S}^1 \times \mathbf{S}^1) \# (\mathbf{S}^1 \times \mathbf{S}^1) \# \ldots \# (\mathbf{S}^1 \times \mathbf{S}^1) \right)}_{n} \ .$$

$$\Updownarrow_{1DL}$$

$$\underbrace{(\mathbf{S}^2 \times \mathbf{S}^1) \# (\mathbf{S}^2 \times \mathbf{S}^1) \# \ldots \# (\mathbf{S}^2 \times \mathbf{S}^1)}_{2n} \ .$$

Proof: The above n^{th}-string presentation produces a manifold with the fundamental group of $\mathbf{S}^1 \times \mathbf{T}_n^2$. This manifold has been shown directly to be this space up to $n = 3$. We conjecture that (a) it holds for each $n \geq 1$ and (b) that the associated 3-gem is the unique with the minimum number of vertices inducing $\mathbf{S}^1 \times \mathbf{T}_n^2$. As a matter of fact it would be very interesting to have a counter-example of part (a) of the conjecture. Thus, we assume it to continue.

We give the proof for $n = 3$, but the argument is entirely general.
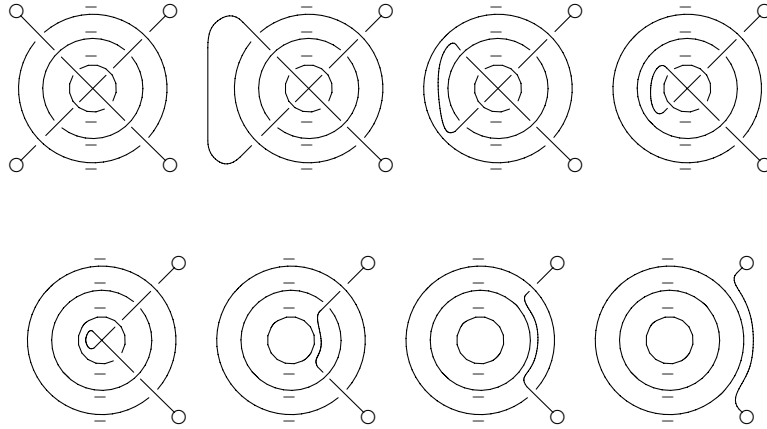
The passage from the first to the second diagram corresponds to a Dehn-Lickorish surgery, see Proposition 22. The next three passages correspond to removal of a non-separating handle. The last three to the removal of separating handles, see Proposition 11. The four connected pieces at the end of the transformations induce $\mathbf{S}^3$'s. ∎

1.3 An Example of Montesinos and Boileau-Zieschang

One of the important findings of last decade was the discovery that the Heegaard genus of a 3-manifold can be greater than the minimum number of generators of its fundamental group. In [BZ84] Boileau and Zieschang displayed an infinite family of 3-manifolds (Seifert spaces) having Heegaard genus 3 whose fundamental group is 2-generated.

The simplest of these manifolds is depicted in the Heegaard diagram below. This diagram, of genus 3 has been obtained by Montesinos, see Fig. 6 of [Mon89]:
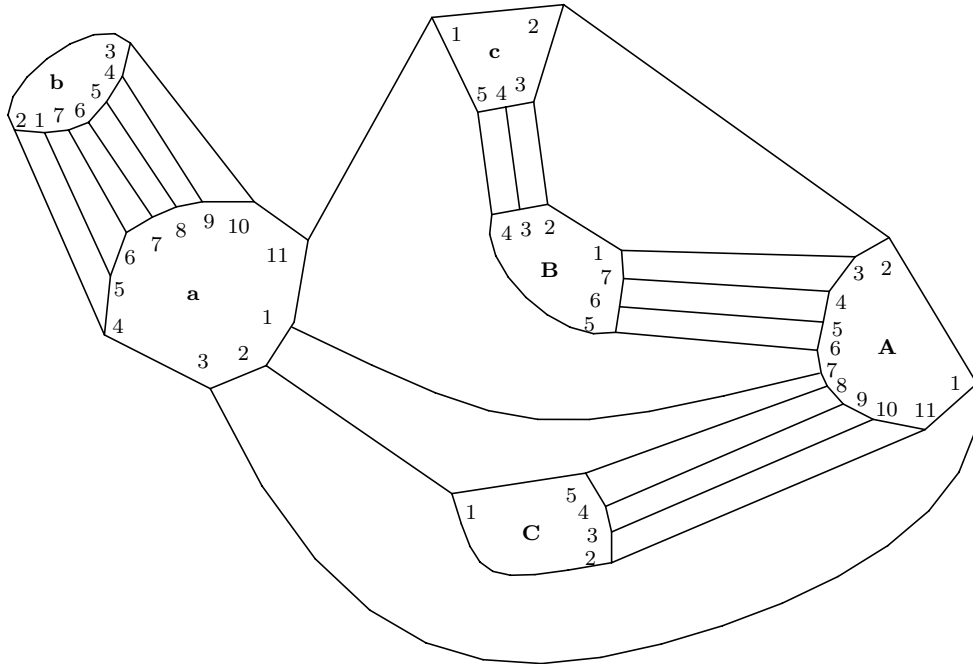
A presentation for the fundamental group of the 3-manifold can be directly read from the Heegaard diagram. It is

$$\langle a, b, c \mid a^2 = (ba^{-1})^2, a = cac, (ba^{-1}c)^3 = (ab^{-1})^2 \rangle \ .$$

As it can be seen, even the first example of the Boileau-Zieschang family is very complicated. As it happen, a simplified 3-gem representing the above 3-manifold admits a string presentation.

To obtain a 3-gem representing the same 3-manifold as the one represented by a Heegaard diagram it is quite easy: double all the edges between the handles; these edges are of colour 1; there exists now, an even number of

edges through each handle; we let the boundary of the disks of the handles to be the 23-gons; the edges of color 0 realize the passage through the handles. The resulting is a $(3+1)$-graph is a 3-gem. It is also easy to show geometrically that the this 3-gem represents the same 3-manifold as the one given by the Heegaard diagram. We leave the details for the reader. This algorithm applied to the above diagram produces a 3-gem with 92 vertices. By using the simplification algorithm with the techniques of [LD91], this 3-gem produces a set of sixteen 3-gems (an *essential TS-class* in [LD91]) each with 32 vertices, all representing the same 3-manifold. The fourteenth 3-gem in this set has a string presentation, which we reproduce below:
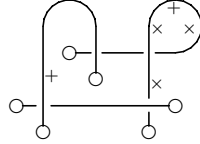
We have included this example here to show that the string presentation, when available, provides a much more compact presentation than Heegaard diagrams. Indeed, it is the internal theory of 3-gems which provides the string presentation: by squeezing as much as we can the 3-gems representing a certain 3-manifold, usually we get symmetric objects, which admit a string presentation.

We do not treat this fact here, but we comment that it is very easy to read a presentation of the fundamental group of a 3-manifold from a string presentation for it; as easy as from a Heegaard diagram.

1.4   The Hyperbolic 3-Manifold with Smallest Known Volume

Consider the following definition of a 4-parametric family of $(3+1)$-graphs $\mathcal{S}(b,l,t,c)$. The vertices are members of $Z_b \times Z_{2l}$. We define four fixed point free involutions β_i, $i = 0, 1, 2, 3$, on the vertices by

$$\beta_0(i,j) = (i + c\mu(j - t), 1 - j + 2t)$$
$$\beta_1(i,j) = (i, j - (-1)^j)$$
$$\beta_2(i,j) = (i, j + (-1)^j)$$
$$\beta_3(i,j) = (i + \mu(j), 1 - j)$$

The arithmetic is mod b in the first and mod $2l$ in the second coordinates. Also the arguments of μ are normalized mod $2l$ to the range $1, 2, \ldots, 2l$. $\mu(j) = 1$ if $1 \leq j \leq l$ and $\mu(j) = -1$ if $l < j \leq 2l$. The edges of $\mathcal{S}(b,l,t,c)$ are these involutions interpreted as colored edges: β_i corresponds to the edges of color i.

Proposition 2 *[Theorem 8 of [LM85]] Let $gcd(b,l) = 1$ and l odd $\Rightarrow c = (-1)^t$. Then the $(3+1)$-graph $\mathcal{S}(b,j,t,c)$ is a crystallization representing an orientable 3-manifold.*

Proposition 3 $\mathcal{S}(3,7,4,1)$ *has the same fundamental group as the fundamental group of the closed hyperbolic 3-manifold with smallest volume known: 0.942707362...*

Proof: A presentation for the fundamental group of this manifold was obtained from J. Weeks (personal communication). He obtained it by doing a Dehn filling in an adequate open 3-manifold with toroidal boundary. [4] [5] In [LS94] we get an isomorphism between Weeks' presentation and a presentation coming from $\mathcal{S}(3,7,4,1)$. These two presentations are given below:

$$\langle a, b \mid a^{-1}ba^{-1}b^{-1}a^{-1}b^{-1}a^{-1}ba^{-1}, ab^{-2}ab^{-2}a^{-1}ba^{-1}b^{-2}\rangle$$

$$\langle x, y \mid x^{-1}yx^{-1}yx^{-2}y^{-2}x^{-1}, y^{-1}x^3y^{-1}xy^{-3}x\rangle$$

We refer the transformations leading from one presentation to the other to [LS94].   ∎

When we apply the simplification procedure of [LD91] (*named $TS\rho$-algorithm*) to $\mathcal{S}(3,7,4,1)$ we obtain a 30-vertex 3-gem (unique in its essential TS-class) which admits a string presentation. This 3-gem and its string

---

[4]By an important result of Mostow [Mos73], the fundamental group of a hyperbolic 3-manifold is a complete invariant, either $\mathcal{S}(3,7,4,1)$ does not admit a hyperbolic metric, or it coincides with Week's 3-manifold.

[5]Recently we got a proof that the two manifolds coincides: from a surgery description on links on S^3 provided by Weeks for the 0.94.. volume manifold we get a 3-gem which also simplifies to the same one as $\mathcal{S}(3,7,4,1)$. Details appear in [Lin95]

presentation are:
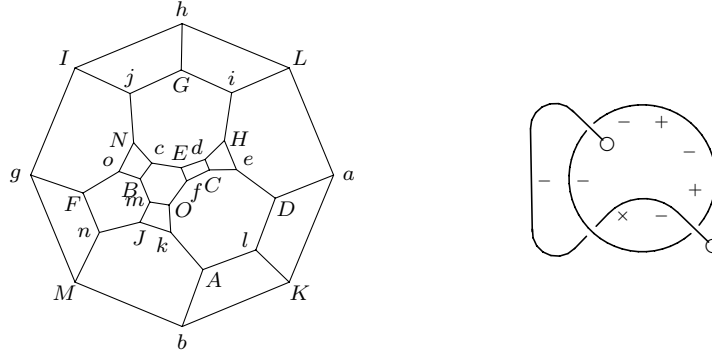
1.5 Elements of the Theory

In this subsection we introduce the basic concepts of string presentations so as to permit the statement of the main results in the next one.

Diagrammatically a *gist* or *string presentation* is a finite collection of open and/or closed curves (named *strings*) embedded in the plane. The restriction on such scheme only will become precise in the next section. Here we introduce and discuss informally the essential aspects in a diagrammatical setting, which will become the main language only in section 3.

Along the strings it may appear three kinds of distinguished points, named *charges* which are of three types: $^+$*charge*, $^-$*charge*, $^\times$*charge*. These are special points on (*attached to*) a string. They are represented by the respective symbol (near the point of attachment). (These "charges" correspond to a pair of fixed points forming an orbit of some special symmetries of the manifold, named σ-symmetries, as defined in the next section.)

Each open string starts and finishes in *endpoints*, or simply *ends*. They are represented in the diagrams by small hollow circles. (They correspond to a fixed point for all the σ-symmetries — see next section.)

A $^\times$*string* is a maximal connected substring which is free of interior $^\times$charges. A $^\times$string is either a closed string or is an open substring bounded by an end and/or a $^\times$charge.

A *segment* is a connected substring free of interior charges and whose extremities is a $\div$crossing (defined below), a charge or an end. (All of our segments are open.)

We permit transversal crossings, however, they are either between exactly two segments or between two pairs of consecutive segments in two $^\times$strings. These $^\times$strings may coincide.

The first type of crossing is a usual one which we name a $^\times$*crossing*. Such $^\times$crossings play a secondary role in our purposes and are only present because we want to remain in the plane. In a higher genus orientable surface, they would not be present.

The second type of crossing is named a $\div$*crossing*. In such a crossing we distinguish a pair of consecutive segments as an *overpass* and the other as an *underpass*. In the diagrams we show which pair is the underpass by removing from it a small interval containing the crossing point, as it is usual in the diagrams for knots and links. (The $\div$crossings corresponds to four points in an orbit of the σ-symmetries — see next section.)

There are four distinct segments incident to a $\div$crossing. By using the cyclic ordering of the incidence given by the planar diagrams, we can partition the four segments into two sets of pairs in three different ways: there are two pairs of *opposite segments*, two pairs of $^+$*angles* and two pair of $^-$*angles*. The definition of opposite segments is self-explanatory. Two consecutive segments form a $^+$angle or a $^-$angle. To distinguish which type, choose an interior point p at a small distance from the $\div$crossing d on the segment of the overpass. Draw an arc with center d and which starts at p towards the segment in the underpass without crossing any segment. If this arc is counterclockwise, the angle is positive, otherwise negative. Below we exemplify this construction, which yields the signs of the four angles incident to a $\div$crossing from the bare $\div$crossing itself:
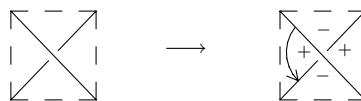
A maximal sequence of segments containing no interior $^+$charges so that each adjacent pair incident to a $\div$crossing is a $^+$angle is called a $^+$*string*. A $^-$string is defined analogously with + replaced by −. Note that while a $^\times$string is entirely contained in the same string, this is not true for $^+$strings or for $^-$strings. However, it will become clear that it is possible to modify the string presentation, (without changing the associated cell decomposition) so as to interchange the *strings and the *strings, where $\star$ and $\ast$ are any two of $+, -, \times$. In this way, there are no abstract differences among the three types.

An *orientation in a gist* is a partition of the ends, the charges and the $\div$crossings into *black* and *white* ones so that each segment has an extremity black and another white. All of our gists are orientable in this sense. [6]

As a general convention, the orientation of the segment is from its black extremity to the white one. A segment belongs to precisely one $^+$string, one $^-$string and one $^\times$string.

To avoid repetitious definitions of concepts, since abstractly there are no differences among the identifiers $+, -, \times$ we use the identifier * to mean a fixed choice of one of them along an argument.

We say that a segment *is *open* or *is *closed* according to whether the type of the *string which contains it is open or closed.

1.6 Overview of the main Results

Suppose a_0 and b_0 are segments belonging to the same closed *string. We say that (a_0, b_0) is **consistent* if going around the *string, the sense of traversal of the segments both agree or both disagree with its orientation (from its black extremity to its white one). If the pair is not *consistent we say that that it is **balanced*. A pair of segments is *open if each segment is *open.

One Theorem which we prove is the following:

Theorem 1 *Let be given a string presentation of a closed 3-manifold M^3. Assume that $(\diamond, \star, *)$ is a permutation of $(+, -, \times)$. Suppose that there exists a pair of segments which is *balanced, *consistent and $^\diamond$open. Then, there is an embedded non-separating torus in M^3 induced by this pair. By removing a small interior interval from each segment and attaching four new ends to the arising four extremities produces a string presentation for another closed connected manifold N^3.* [7]

As an example where this Theorem applies note that the crossing pairs of segments in the presentation for the 3-torus below satisfies the hypothesis of the Theorem. It detects the torus and produces a new closed 3-manifold presented by a gist with more ends. Consider the passage:
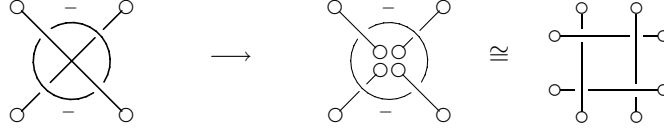
The resulting manifold on the right is a riemannian flat manifold whose fundamental group admits a rigid motion representation. It is labeled $\mathbf{8}_{11}$ in the catalogue of the final section. The presentating gists are distinct. However, there is a string theoretical explanation on why they present the same manifold. It involves changing orientation, disconnecting along a torus and reconnecting. The justifying Theorem relies on Ferri's switching Lemma [Fer87], is called *two mirror property on* 3*-gems* and is the subject of a future paper.

Another example of this kind of torus is induced by the $^\times$crossing segments of the following string presentation of $\mathbf{13}_{21}$:
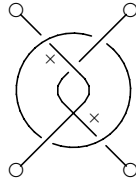
It presents, indeed, a sufficiently large 3-manifold.

On the total, there are 5 types of tori as induced by pairs of segments. We detect them all in section 4. Another basic result which we establish in section 4 is

Theorem 2 *Let be given a string presentation of a prime connected closed 3-manifold M^3. Assume that a pair of segments has the property that removing a small interior interval from each of then disconnects the gist* [8]. *Then, there is an embedded separating torus in M^3 induced by this pair. By attaching four new ends to the severed segments we get two gists presenting connected closed 3-manifolds N_1^3 and N_2^3. Moreover, M^3 can be produced from N_1^3 and N_2^3 by removing from each a solid torus and identifying the boundaries appropriately.*

---

[6]This concept is the manifestation, in the string presentation, of the topological orientability.

[7]At present we do not know but believe that M^3 can be produced from N^3 by removing from it two solid tori and identifying the boundaries appropriately. This type of induced tori is the only one (of the five types induced by pairs of segments) that leaves this doubt.

[8]Note that the $\div$crossings are not disconnecting places. Indeed, the removed intervals from the underpasses are to be considered present for connectivity considerations.

As an application of this Theorem, consider the toroidal decomposition:
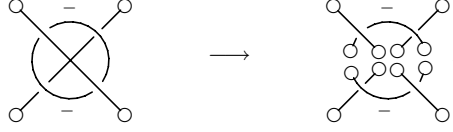
From the theory developed in section 3 it is easy to recognize each of the connected pieces of the gist on the right as presenting a connected sum of the projective 3-space with itself.

This second Theorem is extremely useful in understanding 3-manifolds as toroidal sums of smaller (closed) manifolds. In conjuction with the mentioned 2-*mirror property* this theorem accounts for the *"visual simplification"* of all the string presentations of 3-spheres found in the catalogue [LD89].

The following homeomorphism is justified by the 2-mirror property:
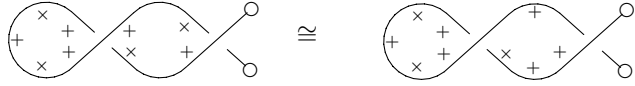
The string presentation in the left comes from a σ-gem (in the catalogue — $R_{28}(149)$) representing $\mathbf{S}^3$. The passage above starts to unlock it. From the theory presented in section 3, the second gist simplifies completely.

It is also possible to see from the gists of the 3-sphere how they are formed by identification of the boundary of complements of knots. For the specific example above consider the simple separation:
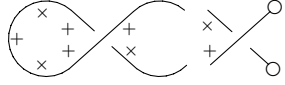
Each one of the gist above (with a pair of severed edges) presents the complement of a knot in $\mathbf{S}^3$. This follows from the fact that the composition presents $\mathbf{S}^3$ and from the theory of manifolds with boundary, presented in section 4.

2 σ-Gems, Expanded Gists and String Presentations

2.1 3-gems

An *(n+1)-graph* is a finite graph G where at each vertex meet exactly $n + 1$ differently colored edges. The total number of colors is also $n + 1$. An *m-residue* is a connected component of a subgraph generated by m specified colors. Note that the 2-residues are even sided bicolored polygons in G, also named *bigons*. Let G^2 be the 2-complex obtained from G by attaching a 2-cell to each 2-residue. A 3-*dimensional graph encoded manifold* or simply a *3-gem* is a 4-graph satisfying the following condition:

$$v + t = b,$$

where v, t, b, stand for the number of 0-, 3- and 2-residues of G. If the above arithmetical condition holds, then each 3-residue with its attached disks form a topological 2-sphere [Lin88]. Let G^3 be the 3-complex obtained from G^2 by attaching a 3-cell to each such 2-sphere. It can be shown that the associated topological space $|G| = |G^3|$ is a closed 3-manifold and that each such 3-manifold arises in this way [LM85]. If a closed manifold M^3 and a 3-gem G satisfy $M^3 \cong |G|$, then we say that G *represents* M^3.

The orientability of the manifold is apparent from any gem G representing it. The manifold is orientable iff G is a *bipartite graph*, i.e., its vertices can be labeled as *black* and *white* so that any edge links a white vertex to a black one (there are no odd cycles (or polygons) in the graph). From the construction for $|G|$ also follows that the interchange of any two colors induces a reversal of orientation and so does the interchange of the black and white classes of vertices.

The colors attached to the edges of a 3-gem are labeled $0, 1, 2, 3$. Two vertices linked by k edges, $(k = 0, 1, 2, 3)$, whose color set is K constitutes a *k-dipole* if they are in distinct components of the subgraph generated by the colors $\{0, 1, 2, 3\} \backslash K$. The *cancellation of a k-dipole* is the following operation: remove the 2 vertices and all k edges between them; this gives $2 \times (4 - k)$ pendant edges; identify pairwise the pendant ends incident to edges of the same color. The inverse operation is named *k-dipole creation*. An *k-dipole move* is either the cancellation or the creation of the dipole.

The diagrams below display the dipole moves for $k = 0, 1, 2, 3$. The colors of the edges are indicated by the number of marks near their extremities. Clearly, the moves are indicated up to color permutations.
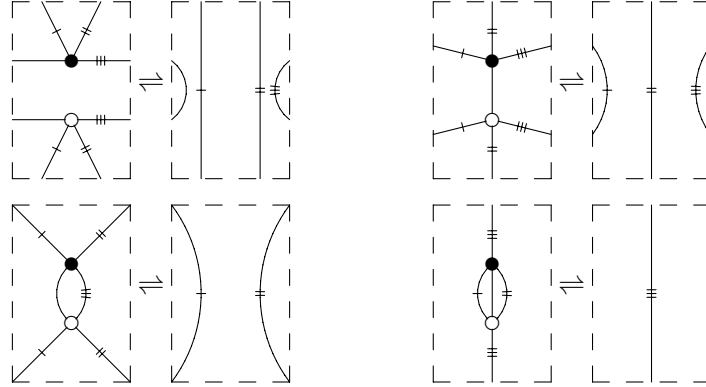
Note that these are not local moves in the sense that we are assuming the exterior connections to imply a k-dipole.

It is not difficult to observe that the k-dipole moves for $k = 1, 2, 3$ do not change the represented manifold, while 0-dipole cancellation is the attachement of a handle. The basic result in the theory of 3-gems is the following Theorem: [9]

Theorem 3 (1- and 2-dipole moves are enough — [FG82]) *If M^3 and N^3 are homeomorphic 3-manifolds, then any 3-gem G_M representing M^3 can be transformed into any 3-gem G_N representing N^3 by means of a finite sequence of 2- and 1-dipole moves.*

There is a dual construction to get the manifold $|G|$ associated to a 3-gem G. [10] Consider a collection of tetrahedra, each with the colors $\{0, 1, 2, 3\}$ labeling its four vertices, in 1-1 correspondence with the vertices of G. For each i-colored edge of G we glue the pair of tetrahedra corresponding to its ends via the triangular face not containing i so as to match the other 3 colors, $\{j, k, l\}$. Do this for every edge of G and the result is a manifold $|G|$, if G is a 3-gem, [Gag79]. This tridimensional dual complex associated to a 3-gem G is denoted G_d^3.

Both constructions are important for the topological interpretation of the fundamental objects and operations in the theory of 3-gems. In fact, it is convenient to consider both dual complexes at hand. We set the following notation to make the correspondence between dual cells:

- a vertex in v in $G \rightleftharpoons$ a solid tetrahedron T_v in G_d^3 whose vertices are labeled $0, 1, 2, 3$;

- an i-colored edge e_i in $G \rightleftharpoons$ a triangular 2-cell E_i in G_d^3 whose vertices are labeled with the 3 colors distinct from i;

- a bigon B_{ij} using colors i, j in $G \rightleftharpoons$ an edge b_{ij} in G_d^3 whose ends are labeled h, k, where (h, i, j, k) is a permutation of $(0, 1, 2, 3)$;

- a 3-residue V_i in G not containing color $i \rightleftharpoons$ a vertex v_i of G_d^3 labeled i.

2.2 σ-Symmetries in 3-Gems

The topological notion of *preserving the orientation*, means, in graphic terms to preserve the bipartition.

A 3-gem G is a σ-*gem* if there are orientation preserving commuting involutions σ^+ and σ^- acting on the vertices of G and inducing automorphisms of G which satisfy:

$$\sigma^+ \text{ interchanges the pairs of colors } (0, 1) \text{ and } (2, 3);$$
$$\sigma^- \text{ interchanges the pairs of colors } (0, 2) \text{ and } (1, 3).$$

As a consequence of the definition, the composition

$$\sigma^\times = \sigma^+ \circ \sigma^- = \sigma^- \circ \sigma^+ \ ,$$

denoted by justaposition, $\sigma^+\sigma^-$, is again an automorphic involution of G, now interchanging the pairs of colors $(0, 3)$ and $(1, 2)$. The orientation preserving pairwise commuting involutions σ^+, σ^- and $\sigma^\times$ are called σ-symmetries.

---

[9]In fact this result is proved in a stronger setting – the crystallization moves – and it is proved for all dimensions. A 3-crystallization is a 3-gem with a minimum number of 3-residues, i.e., four. Any 3-manifold can be represented by a 3-crystallization: just cancell 1-dipoles as long as they are found.

[10]This construction produces the same manifold in the case of a 3-gem G, but it asssociates a topological space to every subgraph to every subgraph of G and so it permits the treatment of some manifolds with boundary (see section 4).

In a way to be made clear, we say that a closed orientable 3-manifold admits a *string presentation* if there is some σ-gem representing it. In fact, we narrow the definition of gists to objects which are in natural 1-1 correspondence with the triples (G, σ^+, σ^-), where σ^+, σ^- make 3-gem G a σ-gem.

Most of the 3-gems that we use to illustrate this exposition are denoted $R_n(m)$. The subscript n is the number of vertices and m is the lexicographic number of order of the *code* for the 3-gem among the *rigid* ([LD89]) gems with n vertices.

An example of a σ-gem is $R_8(1)$, presenting $\mathbf{RP}^3$, whose four 3-residues we display [11] below:
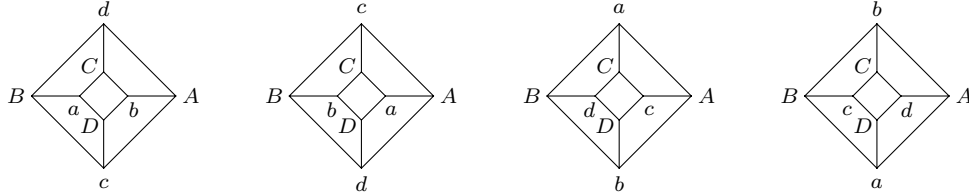
These residues leave out, respectively, colors $0, 1, 2, 3$. The whole 3-gem is recoverable from the first residue because we follow the following conventions. The edges of color 0 link a pair of vertices labeled by the same letter (one lower case, the other upper case — defining the bipartition); the other colors are given by the embedding in the plane, since the bigons are always the boundaries of faces; up to permutation, this defines the colors $1, 2, 3$. To specify the permutation, we make the convention that the outerface of the 3-residue missing the color 0 is a (23)-gon starting counterclockwise at the rightmost vertex. Thus, Ad is 2 colored, Ac is 3-colored (and Ab is 1-colored). This defines colors for all the edges. We use corresponding vertices (by a horizontal translation) in the pictures of the first and the second 3-residues to define the symmetry σ^+:

$$\sigma^+(A) = A \quad \sigma^+(a) = b \quad \sigma^+(B) = B \quad \sigma^+(b) = a$$
$$\sigma^+(C) = C \quad \sigma^+(c) = d \quad \sigma^+(D) = D \quad \sigma^+(d) = c$$

Now use corresponding vertices of the pictures of the first and the third 3-residues to define the symmetry σ^-:

$$\sigma^-(A) = A \quad \sigma^-(a) = d \quad \sigma^-(B) = B \quad \sigma^-(b) = c$$
$$\sigma^-(C) = C \quad \sigma^-(c) = b \quad \sigma^-(D) = D \quad \sigma^-(d) = a$$

Note that they are indeed not only involutions but are automorphisms on $R_8(1)$ of the required type, making it a σ-gem. In particular, we have $\sigma^+\sigma^- = \sigma^-\sigma^+ = \sigma^\times$. See that $\sigma^\times$ is given by the corresponding vertices between the first and the fourth 3-residues:

$$\sigma^\times(A) = A \quad \sigma^\times(a) = c \quad \sigma^\times(B) = B \quad \sigma^\times(b) = d$$
$$\sigma^\times(C) = C \quad \sigma^\times(c) = a \quad \sigma^\times(D) = D \quad \sigma^\times(d) = b$$

2.3 The Expanded Gist

Back to the general case. Suppose that we have a triple (G, σ^+, σ^-), where the σ^+ and σ^- are σ-symmetries of 3-gem G. To derive the string presentation, γ_G, associated to this triple we first define the *expanded gist* Γ_G for (G, σ^+, σ^-). This is the (combinatorial) graph whose vertices are those of G and whose edges are of four types: the original 0-colored edges; edges which link each vertex v of G to $v^+ = \sigma^+(v)$ (these edges may be loops and are labeled with a $+$); edges which link each vertex v of G to $v^- = \sigma^-(v)$ (these edges also may be loops and are labeled with a $-$); edges which link each vertex v of G to $v^\times = \sigma^\times(v)$ (these edges also may be loops and are labeled with a $\times$);

From the expanded gist it is easy to recover the 3-gem. Observe that the colors of a 3-gem may be thought as fixed point free involutions $\{\beta_0, \beta_1, \beta_2, \beta_3\}$ acting on their vertices. Note also that β_0 is the only present in Γ_G. [12]

Proposition 4 *A* 3-*gem is recoverable from any of its expanded gist.*

---

[11] We stress the point that the 3-gems have only labels on the edges (the colors). The reason why we present labeled vertices in the drawings of 3-gems is because this is convenient to represent the action of the σ-symmetries as vertex permutations and also it is a way (together with planarity) to display the colors of the edges (see the text).

Also, the vertex labelings that we present are very special, in the sense that that they are recoverable from the 3-gem itself; see the notion of the *code of a 3-gem* in [LD89].

[12] Of course, any β_i can take the place of β_0 in the definition of expanded gist, in what concerns the recoverability — see its proof.

Proof: To recover a 3-gem G from one of its expanded gist (G, σ^+, σ^-) just note that the color exchanging symmetries means $\sigma^+ \beta_1 = \beta_0 \sigma^+$, $\sigma^- \beta_2 = \beta_0 \sigma^-$ and $\sigma^\times \beta_3 = \beta_0 \sigma^\times$. Since all of the permutations are involutions these equations are equivalent to

$$\beta_1 = \sigma^+ \beta_0 \sigma^+, \quad \beta_2 = \sigma^- \beta_0 \sigma^-, \quad \beta_3 = \sigma^\times \beta_0 \sigma^\times.$$

As β_0, σ^+, σ^- and $\sigma^\times$ are present in the expanded gist, the result follows.   ∎

The $\{\sigma^+, \sigma^- \, \sigma^\times\}$-orbits (corresponding to the connected components of the subgraph of Γ_G generated by $+, -, \times$ labeled edges) may have one vertex, two vertices or four vertices and are called respectively *monopoles, bipoles* and *quadrupoles*. A monopole has three loops attached to it in Γ_G. A bipole corresponds to a subgraph with two vertices in which there are two loops and two non-loops. A quadrupole corresponds to a complete subgraph with four vertices, a K_4.

The gist γ_G is easily derived from any *adequate drawing of* Γ_G, which is basically a free drawing in the plane, as we start explaining.

A monopole is a vertex which is fixed by both (whence the three) symmetries $\sigma's$. A monopole is represented in an adequate drawing of Γ_G by one small hollow circle attached to the unique vertex of the orbit. It becomes then identified with a vertex of the σ-gem. Sometimes we might draw this vertex in black, if is important to display the orientation. Usually however, we use only white ends.

A quadrupole is a K_4 subgraph, in whose vertices the σ-symmetries are transitive and have no fixed points. Each quadrupole is represented in an adequate drawing without the $\times$edges. It becomes a square and is displayed having non-intersecting sides, with the appropriate sign-labels attached to their edges. The closed regions bounded by these squares must be disjoint.

A bipole correspond to a pair of vertices where two of the three σ-symmetries agree (whence the third fixes the two vertices). The bipole is represented faithfully in an adequate drawings for Γ_G, except that we do not need to label the two edges which link the distinct vertices. But we must label the two loops with equal charges. The kind of the charge is given by the kind of σ-symmetry fixing both vertices of the orbit.

The 0-edges of an adequate drawing of Γ_G may $\times$cross transversaly each other or the squares. This finishes our description of adequate drawings of an expanded gist.

To obtain γ_G from an adequate drawing for Γ_G, we start by drawing the diagonals of the quadrupoles with an overpass and a underpass to become a $\div$crossing. The choice for these are according the convention explained in the previous section. We want to delete the signed sides (which are the $^+$angles and $^-$angles of the $\div$crossing) of all the squares corresponding to quadrupoles and yet having a way to recover them.

Following the correct placement of all diagonal we delete all the vertex-labels, all the original edges in the quarupoles and replace the bipoles by one charge equal to the label of their two loops. The result is a string presentation, or gist, γ_G. From it we can recover the expanded gist Γ_G and from this last, the σ-gem G itself.

Observe that an *end* is (combinatorially) defined as a fixed point for all the 3 σ-symmetries. A *charge* is a 2-element orbit of the σ symmetries; the type of the charge is the type of the symmetry which fixes the two elements. A $\div$*crossing* (which corresponds to a quadrupole) is a 4 element orbit of the symmetries, where none of them have fixed point.

Here is an example concerning $R_8(1)$ which we used to illustrate the definition of the σ-symmetries:
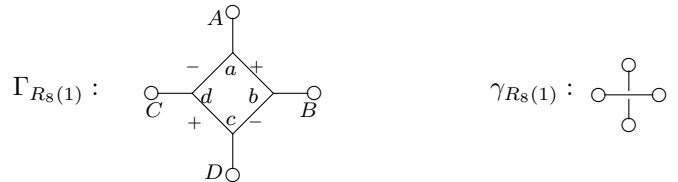
Note that this yields the first string presentation for $\mathbf{RP}^3$. The other two shown in section 1.2 come from other σ-symmetries.

2.4   A Complete Example of Deriving a String Presentation

We give a more representative example of obtaining a string presentation. It will present the quaternionic space and it will have charges, which was not true with the example above.

We begin by displaying σ-symmetries for $R_{18}(1)$, the unique minimum vertex 3-gem which represents $\mathbf{S}^3/Q_8$. All the conventions are like the ones for the case of $R_8(1)$:
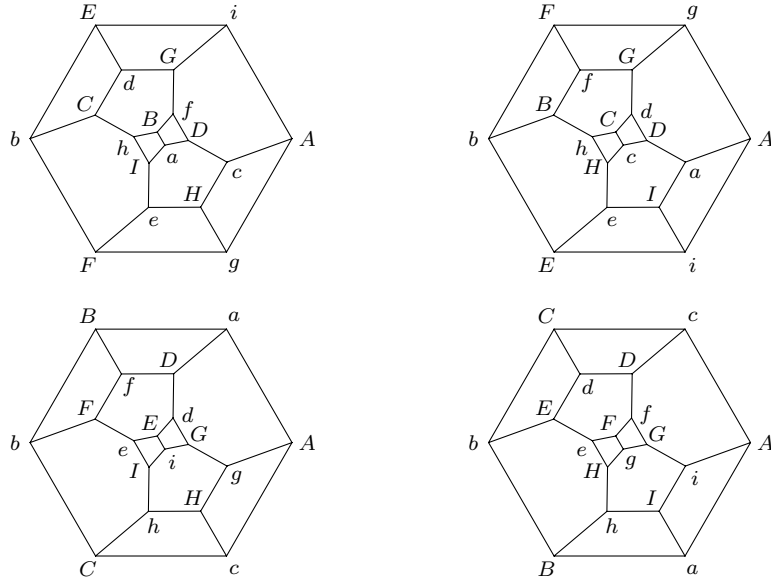
From these σ-symmetries we get an adequate drawing for $\Gamma_{R_{18}(1)}$; we also display $\gamma_{R_{18}(1)}$ after a rotation:
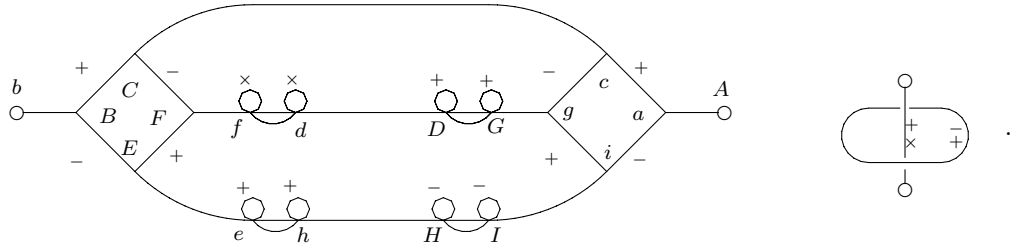
2.5 Exchanging Types of *Strings $\times$ Orientation

Sometimes, by simple change in orientation, is possible to reshape the string presentation to a simpler one. Recall that an exchanging of edge colors is a reversal of orientation. These exchanges are obtained, at the level of the string presentation, by interchanging two types of *strings and preserving the other.

Suppose we want to interchange the $^\times$strings and the $^+$strings while maintaining the $^-$strings. Do some string manipulations creating $^\times$crossings so that for each $\div$crossing there is a $^\times$crossing facing one of its $^-$angles. (That is, the segments of one $^-$angle $^\times$cross.). Gobally *open* all these $^\times$crossings, (as shown below) and interchange the $^+$charges and the $^\times$charges, while maintaining the $^-$charges:
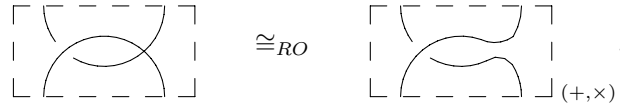
The symbol $\cong_{RO}$ stands for *homeomorphic up to reversion of orientation.*

This global procedure has the effect of interchanging colors 1 and 3 in the associated σ-gem. Therefore, it accounts only for a reversal of orientation.

Of course, if we want to interchange the $^\times$strings and the $^-$strings while maintaining the $^+$strings, just interchange the roles of + and − in the above procedure. To interchange the $^+$strings and the $^-$strings while maintaining the $^\times$strings is easier: just interchange all the overpasses by underpasses in the $\div$crossings and replace the $^+$charges and the $^-$charges while maintaining the $^\times$charges. This means to interchange colors 1 and 2 in the associated σ-gem.

A couple of these manipulations applied to the above example reshape the string presentation obtained in the last subsection to coincide with the first one given for $\mathbf{S}^3/Q_8$, presented in subsection 1.2:
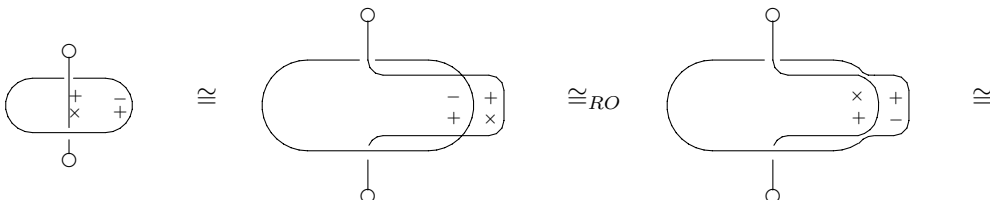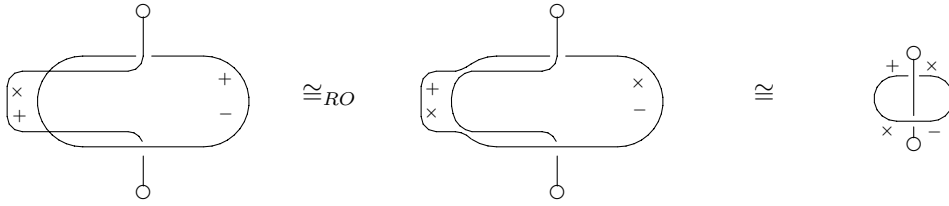
3   Basic Properties of the String Presentation

3.1   General Existence Results

A topologically complete catalog of small 3-gems up to 28 vertices has been produced and classified in [LD89] and [LD91]. The *gem-complexity (or simply complexity) of a closed orientable* 3-*manifold* is defined as one less than half of the vertices of a 3-gem with the minimum number of vertices representing it. From this definition follows that the number of manifolds of a given complexity is finite. [13]

Note that the number of vertices in G equals four times the number of $\dot{\div}$crossings plus twice the number of charges plus the number of ends in γ_G. Therefore, the complexity is apparent in a string presentation.

Up to complexity 13, there are exactly 44 topologically distinct prime orientable manifolds which are not lens spaces (not counting orientation). [14] At present we know that 38 of them admit string presentations. The remaining 6, most likely, also have these presentations. It is true, however, that the 3-gems with smallest number of vertices representing them are not σ-symmetric. This fact already occurs for Poincaré's homology sphere: the unique minimum 3-gem of complexity 11 representing the binary dodecahedral space is not σ-symmetric. The smallest σ-gem representing it is shown below. It has complexity 13 and yields a string presentation for $\mathbf{S}^3/P_{120}$:

$$R_{28}(4079) =$$
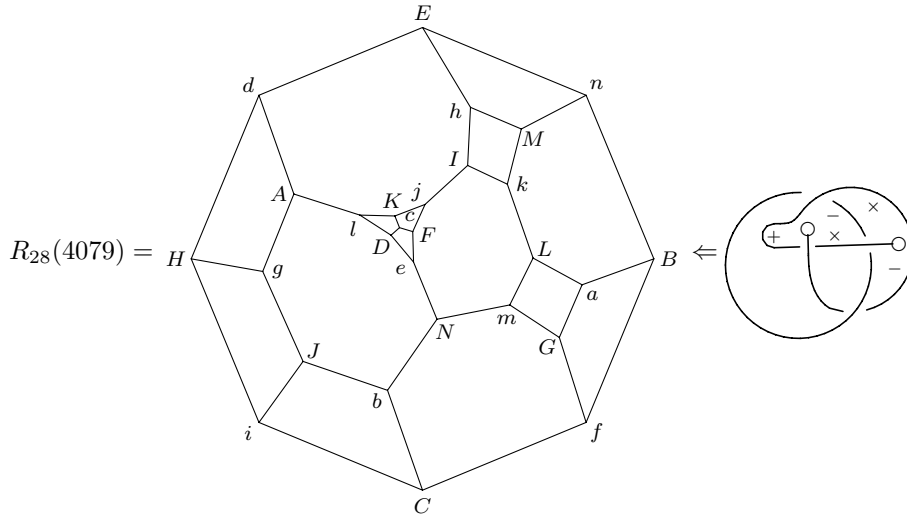
The σ-symmetries of σ-gems imply involutory auto-mappings on the associated manifolds. By a result of Raymond and Tollefson [RT76], there are 3-manifolds without periodic maps. Thus, of course, these manifolds do not admit string presentations. However, they seem to have high complexity and the question of the 3-manifold of smallest complexity which does not admit a string presentation is left open. In general grounds it is easy to prove the following result:

Proposition 5 *Let M^3 be any closed orientable* 3-*manifold. Then, there are string presentations for four disjoint copies of M^3. There are also string presentations for the connected sum*

$$M^3 \# M^3 \# M^3 \# M^3 \# \mathbf{RP}^3.$$

Proof: Let G be any 3-gem representing M^3. Rename it G_0 and make a disjoint copy G_1 of it with the pairs of colors $(0,1)$ and $(2,3)$ interchanged. Make also G_2 by interchanging colors $(0,2)$ and $(1,3)$ and G_3 by interchanging

---

[13]This complexity function seems to be additive on connected sums. In fact, a similar complexity theory by [Mat91] based on *almost special spines* has this property and the proof technique for showing it may apply to 3-gems.

[14]Lens spaces have string presentations and so do connected sums, if the summands have.

$(0,3)$ and $(1,2)$ (relative to G_0). Let H be the gem corresponding to the disjoint union of the G_i's. It is easy to show that H is a σ-gem. Let the vertex v_i of H be the image of the original vertex v in the i-copy. Define

$$\sigma^+(v_0) = v_1 \qquad \sigma^+(v_1) = v_0 \qquad \sigma^+(v_2) = v_3 \qquad \sigma^+(v_3) = v_2 \ .$$

Define also σ^- by interchanging the roles of colors 1 and 2 and $\sigma^\times$ by interchanging the roles of colors 1 and 3. To complete the definition of an expanded gist for Γ_H we just need to define its involution β_0, corresponding to the color 0. This involution is internal to each copy: in copy i it is given by the original color i. This defines the required expanded gist Γ_H. The corresponding string presentation γ_H proves the first part of the Proposition.

The expanded gist $\Gamma_{H'}$ obtained from Γ_H by excising any chosen quadrupole and closing the four severed edges by four ends satisfies the requirement. Let v_i, $i = 0, 1, 2, 3$, the vertices of the excised quadrupole. Suppose that in the original 3-gem G, $\beta_0(v) = w$, $\beta_1(v) = x$, $\beta_2(v) = y$ and $\beta_3(v) = z$. The changes in the expanded gist induce the following local changes to go from H to H':
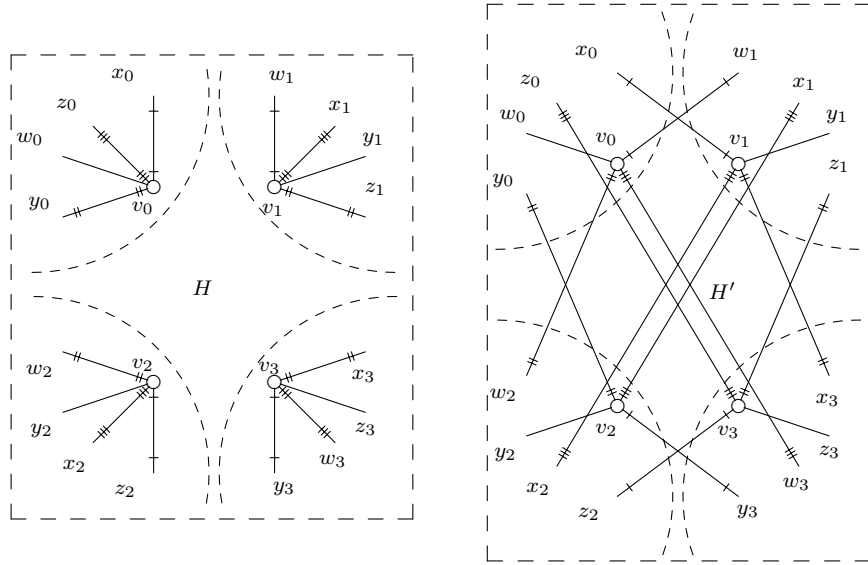
Observe that, in H', by leaving out v_i and contracting the rest of G_i to a single vertex p_i, $i = 0, 1, 2, 3$, we get the canonical *gem* $R_8(1)$ for $\mathbf{RP}^3$. The pairs (v_i, p_i) are 0-dipoles in the 3-gem $H \cup R_8(1)$. Each cancellation of such 0-dipoles corresponds to creating a handle between distinct components. The four cancellations produce H' and the result follows. ∎

The string presentations constructed by the above Proposition basically get us back to the theory of 3-gems. They are almost solely composed of closed strings and usually are difficult to work with. This is because the charges and ends have a much more richer theory.

Proposition 6 (σ-gem of a connected gist) *If a gist is connected, then its associated σ-gem can have one, two or four components. The σ-gem of a connected gist with charges can have at most two components. The one of a connected gist with ends is connected.*

Proof: The proof is easy and is left to the reader. ∎

## 3.2 Simple changes in the string presentations

In this section we analyse simple local changes in a string presentation. They change the manifold only up to handle creations and cancellations.

As we have been doing, we use a dashed box to focus the place of these changes. This means that what goes inside the box is exactly as presented and what goes outside is arbitrary, but fixed throughout an argument. The inside and its implicit extension constitutes a (complete) string presentation, a (complete) expanded gist of a (complete) 3-gem. If any two of these objects (or a symbol like M^3) present homeomorphic 3-manifolds we shall use the symbol $\cong$ between them to indicate that the implicit manifolds are homeomorphic.

**Proposition 7 (Cancelation/creation of a simple linking loop)**

Proof: In the expanded gist, the introduction of the closed ×string corresponds to the introduction of two quadrupoles adjacent by three 0-edges. Note that in the associated 3-gem, this transformation induces the creation of four 3-dipoles. Here are the expanded gist and associated σ-gem asociated to the first string presentation.
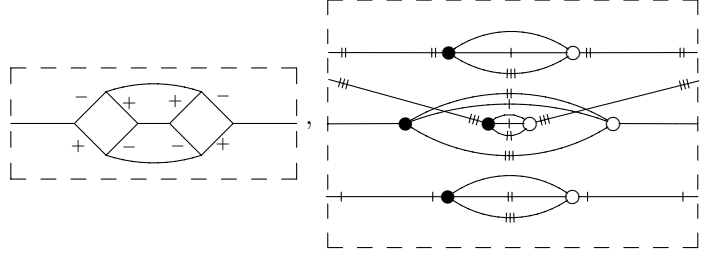
The gem corresponding to the second gist is obtainable from the above one by cancellating these dipoles. Since 3-dipole cancellations do not change the represented manifolds, the property is established.   ∎

Proposition 8 (Dropping/adding a pendant charge) *For an arbitrary* *charge holds in general*
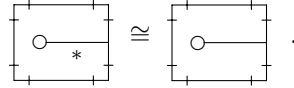
Proof: Assume, without loss of generality, that the *charge is a ×charge. Then, for the first string presentation the expanded gist and associated 3-gem are:
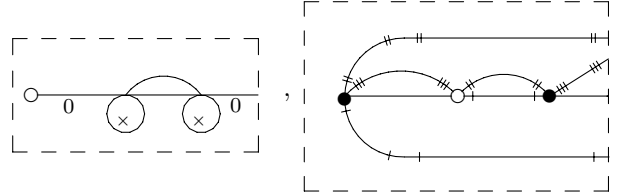
In the σ-gem there are two 2-dipoles, one using colors 1 and 2 and the other using colors 0 and 3. The cancellation of any one of these dipoles corresponds to the dropping of the bipole in the expanded gist, i. e., to the dropping of the charge in the string presentation. This proves the Proposition.   ∎

The general pattern of these proofs are like the two above. Thus, henceforth we leave the verification of the details for the reader, except when the proof involves more than a simple translation between representations.

Proposition 9 (Cancellation/creation of a ×curl) *In general,*
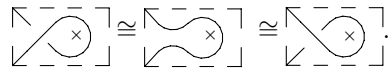
Proof: The proof consists in observing that the move is the manifestation, in the string presentation, of two 2-dipole cancellations in the corresponding σ-gem.   ∎

Recall that to *add a handle* in a manifold M^3 is to remove two disjoint open balls of it and identify the boundaries of these balls by a homeomorphism. Our handles will always be orientable, which means that the identification map opposite orientations for the boundaries of the balls. Note that we are allowing for disconnected manifolds. If the removed balls are in the same component of M^3, then the result of adding a handle is $M^3 \# \mathbf{S}^2 \times \mathbf{S}^1$. If the balls are in distinct components, the addition of a handle produces the connected sum of these components.

If by adding some handles to M^3 produces N^3 then, we write $M^3 \Rightarrow^h N^3$, and also $N^3 \Rightarrow_h M^3$. If N^3 is produced by additions and removals of handles, then we write $M^3 \Leftrightarrow_h N^3$.

Let a and b be differently colored edges of a gem G. We say that $a \equiv b$ if the edges are in the same bigon; otherwise we denote $a \not\equiv b$. In the same way, if they are both i-colored and belong to the same (ij)-gon, then we write $a \equiv_j b$; if they are in distinct (ij)-gons we write $a \not\equiv_j b$. A basic Lemma for many properties is the following:

Proposition 10 (Equivalent σ-symmetric edges) *Let* a_0 *be a segment in a gist* γ_G. *Then* $a_0 \equiv a_0^*$ *if and only if* a_0 *is* *open.*

Proof: The proof follows from the fact that in the expanded gist Γ_G, a closed string corresponds to a $4n$-gon. Going along a pair of edges in a $(0i)$-gon of G, corresponds to follow along 4 edges in the $4n$-gon. Thus, we come back to the origin of the bigon after n such multiple steps. Then, edge a_0^* is not part of the same $(0i)$-gon as a_0. Reciprocally, if the a_0 is open, then all the vertices of the $(0i)$-component of Γ_G that contains a_0 are vertices of a same $(0i)$-gon in G. Then $a_)$ and a_0^* are in the same bigon and so, are equivalent. ∎

The *fusion of a pair of vertices* is the operation in 4-graphs which generalizes the cancellation of dipoles. If the pair has exactly two edges between them, then the fusion is internal to the class of 3-gems, being either a 2-dipole elimination or else the removal of a handle. See [Lin85].

If x_0 is a 0-colored edge of a σ-gem let x_1, x_2 and x_3 be the images of x_0 under the symmetries σ^+, σ^- and $\sigma^\times$, respectively.

Two 3-manifolds *are stably equivalent* if they differ by connected sums with $S^1 \times S^2$.

Proposition 11 (Cancellation/creation of a charge free $^+$link) *The implication*
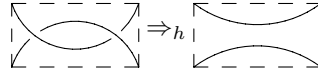
holds in general. There is a homeomorphism if the pair of segments in the second gist is $^+$balanced. If the segments are in distinct components, then the inverse move corresponds to connected sum up to stabilization.

Proof: The implication follows because, at the σ-gems level, we get the second gist by effecting fusion at the of four pairs of vertices with two edges between them that are induced by a charge free link. If the pair is $^+$balanced, call its two segments a_0 and b_0. It follows that $a_0 \equiv b_1$, $a_1 \equiv b_0$, $a_2 \equiv b_3$ and $a_3 \equiv b_2$. Creating four 2-dipoles by subdividing each one of these equivalent pairs of distinctly colored edges we get a σ-gem corresponding to the first gist. ∎

Proposition 12 (Dropping/adding a pair of equal charges) *For an arbitrary charge $*$ it holds in general the implication*
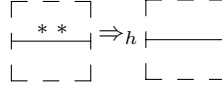
*The homeomorphism holds if the segment in the second gist is *open.*

Proof: The pair of equal charges induce a couple of pairs of vertices with two edges between them. By effecting fusion at these pairs we get the Proposition. ∎

The following Proposition is often useful to simplify string presentations:

Proposition 13 (A nine-vertex Lemma)
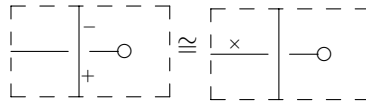
Proof: The first configuration implies, in the σ-gem, a cluster of four bigons in a 2×2 disposition having all the nine vertex distinct, as shown in the left gem below. The central vertex corresponds to the end of the first gist. The nine vertices being distinct, by 2-dipole and 1-dipole moves the configuration is transformed into the one shown in the right, which corresponds to the second gist.


∎
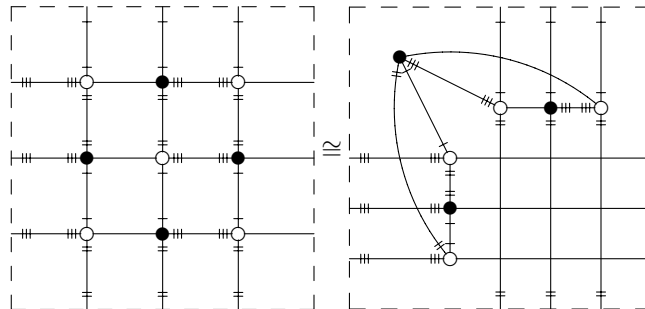
3.3 Quadricolors and String Presentations

In this subsection and the next ones we gather the basic facts about gists and their interconnection with Dehn-Lickorish surgeries. In 3-gems these surgeries have a very simple combinatorial manifestation, operations on *quadricolors* – in this subsection and on *mutants* – in the next subsection. These objects are often inherited by the string presentations.

A *quadricolor* of a 3-gem is a polygon formed by four differently colored edges. There are three simple operations which we can perform on quadricolors. These operations are internal to the class of 3-gems [Lin89] and are named: the *smoothing of a quadricolor* or Q_s; the *reversal (of orientation) of a quadricolor* or Q_r; the *antipodal identification of a quadricolor* or Q_i. These operations are defined by the passages:
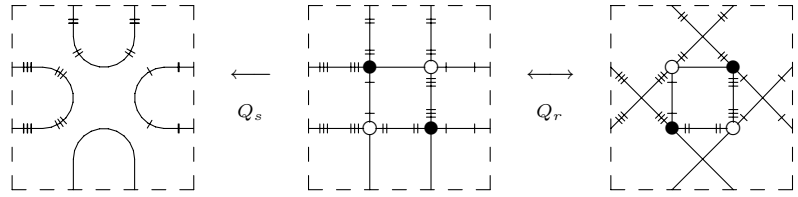
and
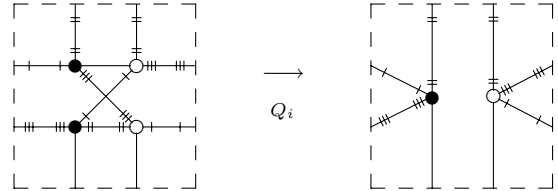
The following Theorem is proved in [Lin89]

Theorem 4 (Q_s and Q_i are universal) *Q_s and Q_i are internal to the class of 3-gems. Any of these operations in conjunction with the 2- and 1-dipole moves is capable of transforming any 3-gem representing any closed orientable 3-manifold into any other 3-gem representing any other such manifold by a finite sequence of moves.*

The inverse operations of Q_s and Q_i are not always available in the sense that they can produce non-gems (which induce pseudo-manifolds with singularities by the dual construction). Therefore, we avoid using them completely. The operation Q_r, however is of involutory type, and so its inverse is at hand.

In G_d^3, a quadricolor corresponds to an embedded solid torus, T_Q, formed by four tetrahedra and having eight triangular faces forming its boundary. Below we stack the four tetrahedra forming a solid cylinder. It becomes a solid torus when we identify the lower base, a_1, and the upper one, d_1. Thus, under geometric duality we have the correspondence:
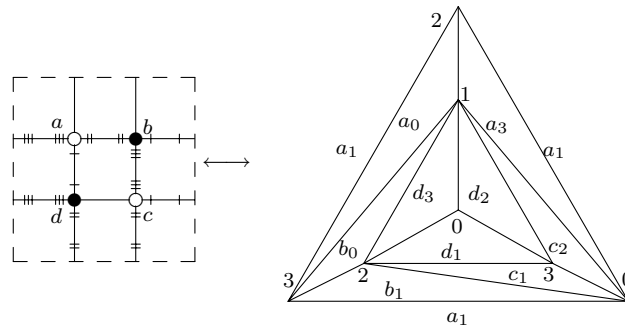
Relative to the triangulation of its boundary, the simplest embedding of the surface of T_Q into R^3, is one for which the *meridian curve*, i.e., the curve which is contractible in the solid torus but not in its surface, becomes a curve of type $(1, \pm 1)$. The convention is that a canonically embeddeded solid torus has meridian of type $(0, 1)$.

Here is the boundary simplest embedding in R^3 of ∂T_Q and the effect of Q_i in the dual complex G_d^3: Note that the meridian curve (in the manifold) of the solid torus T_Q is formed by the 3 edges between the faces a_0 and c_1, a_3

and d_3, b_1 and d_2.
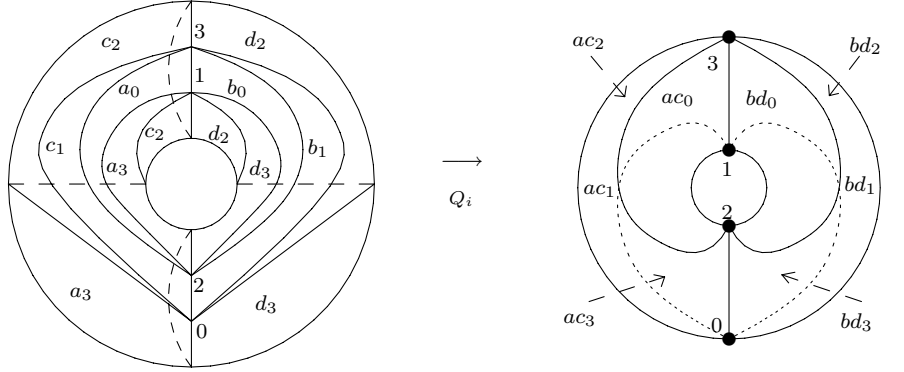
The two tetrahedra corresponding to the identified vertices have opposite orientations and exactly two opposite edges in common. Such a configuration is called a *balanced $^-$hinge* . Note that the regular neighborhood of a hinge is a solid torus. Note also that T_Q and the hinge $Q_I(T_Q)$ have the same boundary.

The two vertices that corresponds to a balanced ^-hinge are in the same 02-gon, in the same 13-gon and in distinct 01-, 03-, 12- and 23-gons. Such pair of vertices is named a $^-antipole$. There are also $^+antipoles$ and $^\times antipoles$, defining by interchanging colors $(2,1)$ and $(2,3)$. Operation Q_i followed by fusion at the resulting antipole is equivalent to Q_s. The operation of antipole fusion is denoted A_f.

Theorem 5 (Antipole fusions are universal $-$ [Lin89], [Lin92]) *A_f is internal to the class of 3-gems. In conjunction with the 2- and 1-dipole moves A_f is capable of transforming any 3-gem representing any closed orientable 3-manifold into any other 3-gem representing any other such manifold by a finite sequence of moves.*

We observe that the operations A_f, Q_s or Q_i correspond to 2-dipole moves and one Dehn-Lickorish surgery [Lin89]. This surgery is defined as follows. A solid torus is removed from the manifold and its triangulated surface is canonically embedded into R^3 so that the meridian curve is faithful, i.e., of type $(0,1)$. Consider now a solid torus with an isomorphic triangulation in its boundary, canonically embedded in R^3 so that the meridian curve is either of type $(1,\pm1)$ or $(1,0)$. This solid torus is glued back in the manifold.

The proofs of the above Theorems, which are 3-gem counterparts of [Lic62], are made from first principles and do not need to consider a generator set for the mapping class group of the orientable surfaces.

If the manifold M^3 produces another N^3 by at most n Dehn-Lickorish surgeries realized by smoothing of quadricolors, then we write $M^3 \underset{nQ_s}{\Rightarrow} N^3$. If the Dehn-Lickorish surgeries are realized by antipodal identifications of quadricolors, then we write $M^3 \underset{nQ_i}{\Rightarrow} N^3$. This is only to be more specific, since, up to 2-dipole moves, Q_s and Q_i are equivalent [Lin89]. Using these notations we mean that the implications are without 2-dipole moves.

The following Theorem is also proved in [Lin89]

Theorem 6 (Q_r is Z_2-universal) *Q_r is internal to the class of 3-gems and preserves the homology mod 2. In conjunction with the dipole moves it is capable of transforming any 3-gem representing any Z_2-homology sphere into any other 3-gem representing any other Z_2-homology sphere by a finite sequence of moves.*

In fact, Q_r corresponds to a torus surgery, in which a solid torus is removed and its surface is canonically embedded into R^3 so that the meridian curve becomes of type $(1,1)$. Consider now a canonically embedded solid torus with isomorphic triangulation in its boundary so that the meridian is the curve $(1,-1)$. This is the solid torus that we glue back in the manifold. Name these surgeries *even Dehn-Lickorish surgeries* .

If the manifold M^3 produces another N^3 by at most n even Dehn-Lickorish surgeries produced by Q_r's we write $M^3 \underset{nQ_r}{\Leftrightarrow} N^3$.

A connection between Q_r and the string presentation is given by

Proposition 14 (Interchanging adjacent pair of distinct charges) *Let $*$ and $\star$ denote different charges. Then*

$$\boxed{\;*\;\star\;} \underset{1Q_r}{\Leftrightarrow} \boxed{\;\star\;*\;} .$$

Proof: The pair of charges corresponds to a quadricolor in the associated σ-gem. Interchanging the pair of charges corresponds to reversing (the orientation) of the quadricolor.   ∎

A first connection between Q_s and string presentations is given by

Proposition 15 (Dropping adjacent pair of distinct charges) *Let $*$ and $\star$ denote different charges. Then*

$$\boxed{\;*\;\star\;} \underset{Q_s}{\Rightarrow} \boxed{\qquad}\;.$$

The inverse implication holds if the segment is both *open and *open.

Proof: The pair of charges corresponds to a quadricolor in the associated σ-gem. Dropping the pair of charges corresponds to smoothing the quadricolor. Reciprocally, if the segment is *open and *open then we can create a pairs of adjacent *charges followed by a pair of adjacent *charges, as proved in last subsection. Then use the first part to drop the medial pair of adjacent distinct charges.   ∎

A first direct use of use of Q_i to the string presentation is given by

Proposition 16 (Breaking a fake link) *In general,*

$$\underset{2Q_i}{\Rightarrow}\;.$$

The inverse implication is not true in general.

Proof: The fake link induces two quadricolors in the associated σ-gem. By effecting Q_i at these we get the Proposition.   ∎

It is interesting to observe that, on the contrary of knot theory, the fake link is the one that provides topological difficulty: it seems to need two Dehn-Lickorish surgeries to be undone. Compare this with the removal of a real link, as we treated before.

Proposition 17 (Cancelling/creating a fake link) *In general,*

$$\underset{2Q_s}{\Rightarrow}\;.$$

The inverse implication holds (by first creating eight 2-dipoles) if the pair of segments in the second gist is simultaneously $^+$balanced and $^-$balanced.

Proof: The fake link induces two quadricolors in the associated σ-gem. By effecting Q_s at these we get the implication. Conversely, if the pair is $^\pm$balanced then we can create a $^-$link and a $^+$link, which do not change the homeomorphism type. After that we use the first part to remove the central fake link.

$$\cong \underset{2Q_s}{\Rightarrow}\;.$$

                                                                 ∎

The breaking or/and cancelling of a fake link is maybe the only place to start unlocking some string presentations. Consider the one below:
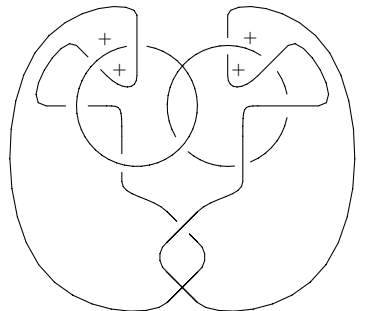
This gist is a presentation of the 2-fold branched covering of $\mathbf{S}^3$ where the branching set is the alternating link over the medial of the 1-skeleton of the cube. In the language of [Lin88], this manifold is $\Psi\left(\;\boxed{\boxtimes}\;\right)$.

A sufficient condition to have the converse of the above property, which is useful in deriving the next Propositions is

**Proposition 18 (String pulling at a $^+$angle)** *If the $^+$angles at the leftmost $\div$ crossing below are $^-$balanced, then,*
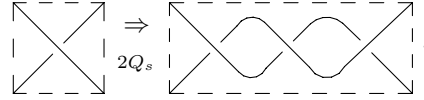
Proof: The hypothesis imply that the segments of the ^+angles are $^\pm$balanced, since the segments in a $^+$angle are obviously $^+$balanced. ∎

With the above facts settled, it is easy to prove the following two properties:

Proposition 19 ($^+$Fissionable $\div$crossings) *The $^+$fission of a $\div$ crossing into two $^\times$charges*
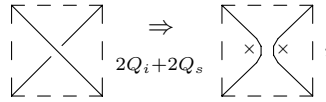
holds if the $^+$ angles of the $\div$crossings are $^-$balanced.

Proof: Pull the string at the rightmost $^+$angle, break the fake link and remove the $^\times$curl. ∎

Proposition 20 (Switching a $\div$crossing) *If the $^+$angles are $^-$balanced in the $\div$ crossing of the first gist, then*
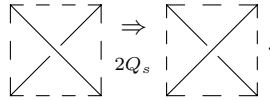
The inverse implication is only true if the $^-$angles displayed in the first gist are in distinct $^-$strings.

Proof: Pull the string at the rightmost $^+$angle and cancell the $^+$link formed. If the hypothesis for the converse is not true, then the inverse move would create a non-manifold. If it holds, the situation is symmetric in $(+,-)$. ∎

3.4   Mutants

A ^+mutant in a bipartite 3-gem is a pair of vertices which are in the same class, in the same 01-gon, in the same 23-gon and in distinct 02-, 03-, 12- and 13-gons.

To define a ^-mutant and a $^\times mutant$ interchange the roles of the pairs of colors (1,2) and (1,3), respectively.

Proposition 21 (Mutations) *The pair of vertices in the first 3-gem below is a ^+mutant if and only if the pair in the second is a ^-mutant if and only if the pair in the third is a $^\times mutant$. Moreover any pair of the three 3-gems below represent 3-manifolds obtainable one from the other by one Dehn-Lickorish surgery:*
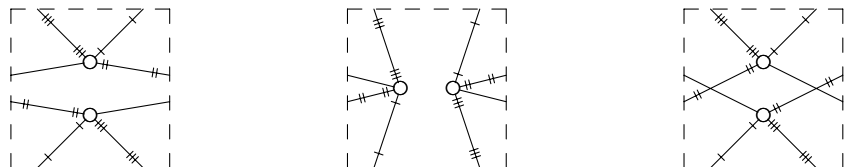
Proof: A *mutant corresponds to a *consistent *hinge* under geometric duality: two tetrahedra of the same orientation, having a pair of opposite edges in common. The consistent $^+$hinge, $^-$hinge and $^\times$hinge are:
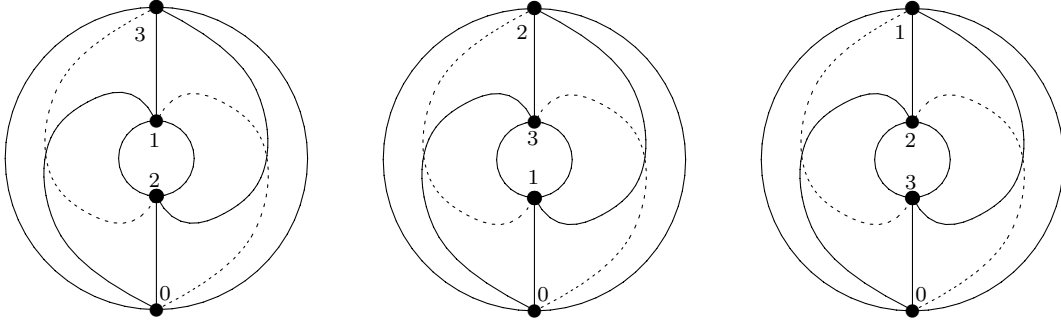
The result follows directly from the connectivity hypotheses over the bigons and the dual geometric interpretation.
■

Mutation is also a very basic operation:

Theorem 7 (Mutations are universal – [Lin92]) *Mutation is internal to the class of 3-gems. In conjunction with the 2- and 1-dipole moves a finite number of mutations is capable of transforming any 3-gem representing any closed orientable 3-manifold into any other 3-gem representing any other such manifold by a finite sequence of moves.*

Some basic connections between mutants and gists are given by the two Propositions below. A charge is called *open if the segments that contain it are *open. It is $^\diamond$closed if these segments are $^\diamond$closed.

Proposition 22 (Fissioning or Mutating an *open *charge) *If a *charge in a string presentation is *open and $^\diamond$closed, then it is fissionable into two ends or it can mutate to a *charge by one even Dehn Lickorish surgery:*

Proof: The direct and inverse moves in the two situations are precise manifestations of the two possible mutations.
■

We conclude this section with a move which has not yet a clear topological interpretation. However it is the *attachment of a 3-torus* (in a strange and maybe canonical way) to another 3-manifold; a kind of generalized handle creation. [15]. By its simple manifestation in the string presentation it might turn out to be a relevant move.

Proposition 23 (Strange attachment of a 3-torus) *Assume that the $^\times$crossing pair of segments in the first gist below is $^+$balanced, $^-$consistent and $^\times$open. Then the move depicted below yields another string presentation for some other 3-manifold.*
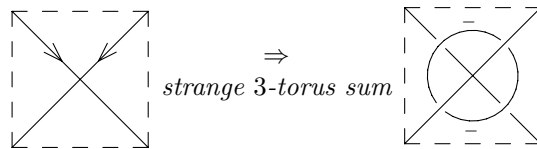
The converse move holds if the $^\times$crossing pair of segments in the second gist is $^-$balanced, $^+$consistent and $^\times$open.

**Proof:**   Ommitted.   ■

4   Decompositions along Spheres and Tori

In this section we get some results on the detection of spheres and tori in string presentations.

---

[15]In the sense that handle creation is the connected sum with $\mathbf{S}^2 \times \mathbf{S}^1$, this operation is some type of sum with $\mathbf{S}^1 \times \mathbf{S}^1 \times \mathbf{S}^1$

4.1   Manifolds with Boundary

We want now to consider manifolds with boundary so that each component is either a torus or a sphere. The string presentation, via the associated 3-gems, can deal with such manifolds. To do it we use the dual construction leaving out some tetrahedra or avoiding doing some identifications. For instance, given a 3-gem G and any vertex v we can remove T_v and have a 3-manifold whose boundary is an sphere. We represent this operation by surrounding the v with dots. If G is a σ-gem and v is an end, this notation is extended to the gist $\gamma(G)$:
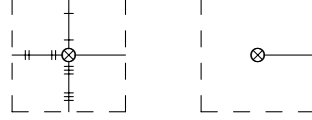
A segment in a string presentation is called *all open* if it is $^+$open, $^-$open and $^\times$open. An *isthmus* in a graph is an edge whose deletion increases the number of connected components. We extend this terminology to gists.

Proposition 24 (All open segments and embedded spheres) *An all open segment (an isthmus, in particular) in a string presentation γ_G induces an embedded sphere in $|G|$. Thus in a minimal string presentation of a prime manifold, the only all open segments are the ones adjacent to ends.*

Proof: Let a_0 be the segment. Then a_0, a_1, a_2, a_3 are two by two in the same bigon and A_0, A_1, A_2, A_3 (in the dual complex G_d^3) form the surface of tetrahedron, which is topologically a sphere. [16]   ∎

The cutting of such an sphere means not to identify the four triangular faces induced by the segment. The situation is described in a string presentation by surrounding an interval of the segment with a dotted box:
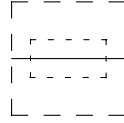
A segment which is severed in the above way means that it is an all open one. Also, we make the convention that a gist like this is presenting the manifold with two sperical boundary components obtained (from the one presented without the dotted box) by cutting the sphere induced by the segment.

The following Proposition is used in proving that some 4-graphs are 3-gems. The *agemality* of a 4-graph G is the integer $\alpha_G = v_G + t_G - b_G$.

Proposition 25 (Non-negativity of agemality − [LM85]) *The agemality of any 4-graph is non-negative.*

All the surrounded vertices and intervals are explicitly displayed inside the focus of our attention, the dashed boxes. If there is more than one, say n, vertices surrounded, the associated tetrahedra must be pairwise disjoints and the associated σ-gem has at least $4n$ 3-residues. With these conventions, here is an statement about producing a manifold with two spherical boundary components in two distinct ways:

Proposition 26 (Cutting a sphere $\times$ creating a handle) *The segment in the first gist below is all open if and only if the tetrahedra corresponding to the vertices in the second are disjoint and holds:*
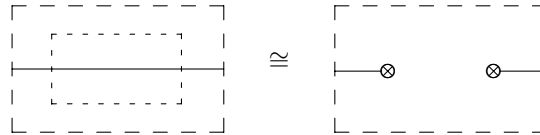
Proof: Let G be the 4-graph associated with the first string presentation and G' the one associated with the second. Note that $v_{G'} = v_G + 2$, $b_{G'} = b_G + 6$ and that the separation of the vertices imply at most one more 3-residue of each type, that is, $b_{G'} \leq b_G + 4$. Since the agemality is non-negative, we have the converse inequality. $b_{G'} \geq b_G + 4$ and the result follows.   ∎

Recall that a mutant or an antipole in a 3-gem G (see last section) induces a solid torus in $|G|$: the pair of tetrahedra corresponding to the mutant or to the antipole has a pair of opposite edges in common; its regular neighborhood is an embedded solid torus. Removing this solid torus is accomplished by leaving out the pair of

---

[16]This surface can be bounding, if the segment is incident to an end; it can be separating and non-bounding, if is not incident to an end but is an isthmus; it can also be non-separating.

tetrahedra from the dual construction. Removing such solid tori is depicted in diagrams for gems and gists by surrounding the pair of vertices by a dotted box. Often antipoles and mutants in σ-gems are formed by pair of vertices which are ends in a gist. Also, a mutant often manifests itself as a charge (which, after all is a pair of vertices in the same class). We display the cutting of a charge by surrounding it together with intervals of the supporting segments by a dotted box, see the statement of Theorem on the diagrammatic cutting of tori, which comes after the next one.

4.2 Detecting Embedded Tori in String Presentations

We say that a pair of segments (a_0, b_0) in γ_G induces a torus if

$$\{A_0, B_0, A_1, B_1, A_2, B_2, A_3, B_3\}$$

is an embedded torus in $|G|$. We display the cutting of this torus by surrounding intervals of the segments with a dotted box.

There are five types of tori which are induced by pairs of segments. All of these types do occur.

Theorem 8 (Induced tori) *A pair of segments (a_0, b_0) in γ_G induces an embedded torus in $|G|$ if and only if the pair is, up to permutation of $+, -, \times$, one of the following types:* [17]

1. $^{+}$*open,* $^{-}$*open and* $^{\times}$*balanced;*

2. $^{+}$*open,* $^{-}$*open and* $^{\times}$*consistent;*

3. $^{+}$*balanced,* $^{-}$*balanced and* $^{\times}$*balanced;*

4. $^{+}$*balanced,* $^{-}$*balanced and* $^{\times}$*consistent;*

5. $^{+}$*balanced,* $^{-}$*consistent and* $^{\times}$*open.*

Proof: The proof that only these types produce tori is done by considering all the possibilities. It is tedious and we give full details only in the first case. From the proof of the first case, one can treat all the other cases similarly and conclude that the cases not listed do not produce tori.

Here are the induced 2-subcomplexes in the five cases, in the same order in which they are listed. Note that they close as a torus in each case. We need to be carefull to show that there are no spurious identifications. Indeed, all the four vertices and the twelve edges are distinct in each one of the five cases:
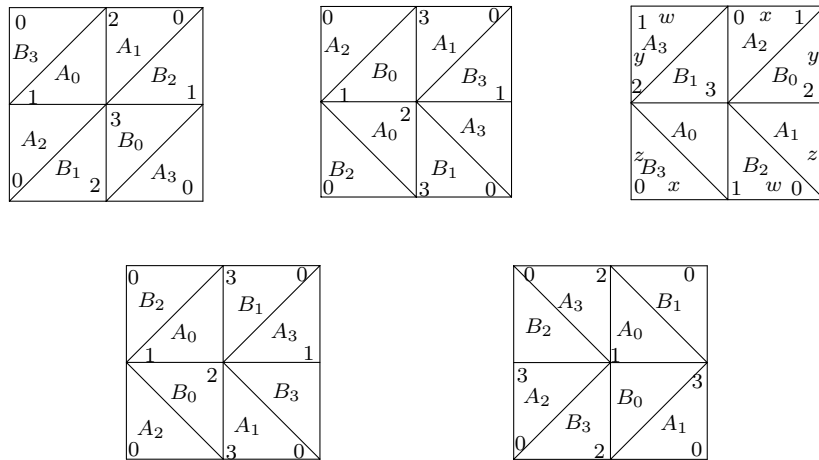
We may suppose, without loss of generality that the segments in an *open pair are in distinct *open strings. If not we can subdivide the string by attaching an adjacent pair of *charges which accounts for 2-dipole moves and accomplishes this hypothesis.

Follows a detailed proof for the first type. All the equivalences and non-equivalences among the eight edges induced by the pair are given in the table below:

---

[17]As we shall show, only the last type leads to some difficulty in presenting the manifold with double toroidal boundary by cutting along the torus

	b_0	a_1	b_1	a_2	b_2	a_3	b_3
a_0	$\neq_1 \neq_2 \neq_3$	$\equiv$	$\neq$	$\equiv$	$\neq$	$\neq$	$\equiv$
b_0		$\neq$	$\equiv$	$\neq$	$\equiv$	$\equiv$	$\neq$
a_1			$\neq_0 \neq_2 \neq_3$	$\neq$	$\equiv$	$\equiv$	$\neq$
b_1				$\equiv$	$\neq$	$\neq$	$\equiv$
a_2					$\neq_0 \neq_1 \neq_3$	$\equiv$	$\neq$
b_2						$\neq$	$\equiv$
a_3							$\neq_0 \neq_1 \neq_2$

The entries in the first row of this table are justified as follows:

$$a_0 \neq_1 b_0 \Leftarrow a_0, b_0 \text{ are in distinct } {}^+\text{strings};$$
$$a_0 \neq_2 b_0 \Leftarrow a_0, b_0 \text{ are in distinct } {}^-\text{strings};$$
$$a_0 \neq_3 b_0 \Leftarrow (a_0, b_0) \text{ is } {}^\times\text{balanced};$$
$$a_0 \equiv a_1 \Leftarrow a_0 \text{ is } {}^+\text{open};$$
$$a_0 \neq b_1 \Leftarrow a_0, b_0 \text{ are in distinct } {}^+\text{strings};$$
$$a_0 \equiv a_2 \Leftarrow a_0 \text{ is } {}^-\text{open};$$
$$a_0 \neq b_2 \Leftarrow a_0, b_0 \text{ are in distinct } {}^-\text{strings};$$
$$a_0 \neq a_3 \Leftarrow a_0 \text{ is } {}^\times\text{closed};$$
$$a_0 \equiv b_3 \Leftarrow (a_0, b_0) \text{ is } {}^\times\text{balanced};$$

To get the second row we interchange the a_i's and the b_i's. We get the third row from the first by using symmetry σ^+. We get the fourth row from the second by using symmetry σ^+. We get the fifth row from the first by using symmetry σ^-. We get the sixth row from the second by using symmetry σ^-. Finally, we get the three entries for the seventh row from the first by using symmetry $\sigma^\times$. The equivalent and non-equivalent edges mean adjacent and non-adjacent triangular faces in G_d^3. Whence, the subcomplexes that we show is a direct translation from the above table.

Note in particular that its twelve edges are distinct, because there are twelve distinct bigons (two of each type) incident to the eight edges appearing in the table. The four vertices of the subcomplex are distinct: they correspond to 3-residues which leave out a colors 0, 1, 2 and 3. Thus, the first type is established. The others are entirely similar. ∎

The pair of segments corresponding to the the first gist in the Theorem below is $^+$balanced, $^-$open, $^\times$open if and only if the surrounded pairs of vertices in the right one corrrespond to disjoint mutants. If one of these equivalent facts holds, then the pair on the left induce an embedded torus. Moreover cutting along the torus on the closed manifold at the left produces a manifold with a two component toroidal boundary which is homeomorphic to the manifold obtained from the closed manifold at the right by removing a pair of disjoint solid tori corresponding to the pair of mutants. Note that this previous phrase is contained in our conventions for associating dotted boxes to manifolds with boundary. For the other cases, we let the diagrams speak

Theorem 9 (Diagrammatic cutting of tori)

A torus of the type 1 implies:

A torus of type 2 implies:

Tori of types 3 or 4 imply:
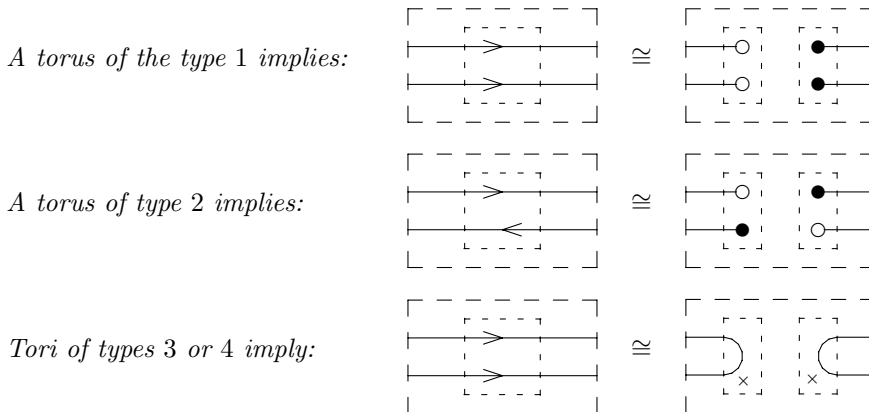
Moreover, these tori are separating if and only if the operation on the string preseentation increases the number of its connected components.

Proof: The proof is basically a careful count on the number of vertices, bigons and 3-residues of the closed manifold associated to the gists on the right. In each case, by making use of the non-negativity of the agemality,

we establish the balance $v + t = b$. Follows, in particular, that all the 3-gems associated to the string presentations on the right have four more 3-residues than the corresponding on the left. Thus the solid tori associated with the surrounded mutants, antipoles and charges are disjoint and the representation is faithful: cutting the torus yields manifolds with a double toroidal component, obtained by leaving out, in the dual construction, the eight sixteen identifications corresponding to the 2×8 severed edges (induced by removing the two intervals in the dotted box). ∎

For the last type of torus we would like to say that: If the pair below is $^{+}$balanced, $^{-}$consistent and $^{\times}$open then,
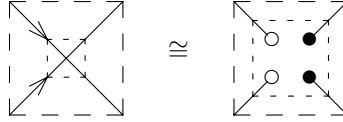
However, leaving out the four tetrahedra in the construction of the gist on the right produces a pseudo-manifold with a complicated boundary, which is not a surface. The root of the difficulty is that in this case the number of 3-residues in the passage from the first closed manifold to the second does not increase the number of 3-residues. It is however a fact that the result of the strange operation of the torus produces a closed manifold:

Theorem 10 (Operating on tori of the fifth type) *A pair of segments which is $^{+}$balanced, $^{-}$open, $^{\times}$balanced induces a non-separating torus. The passage,*
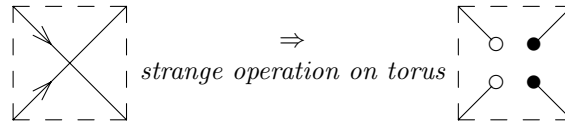
produces a closed 3-manifold obtained by cutting along the torus and closing the resulting manifold in the canonical way suggested by the string presentation.

Proof: The proof follows by counting residues as in the previous one. The fact the the torus is non-separating follows because in the resulting gist the four new ends are vertices of the associated σ-gem which are in the same 3-residue not using color 3. Then the number of 3-residues is invariant. ∎

For the following Theorem the symbol $\Rightarrow_{ht}$ means that the second gist presents a 3-manifold obtained from the one presented by the first after a cutting along spheres (related to *h*andle removal) or *t*ori and closing the 3-manifolds with boundaries in the canonical way.

Theorem 11 (Splitting at a disconnecting pair) *Suppose that a gist minimally presenting a connected prime 3-manifold has a pair of segments whose deletion disconnects it. Then, this pair induces a handle or torus and exactly one of the following implication holds:*
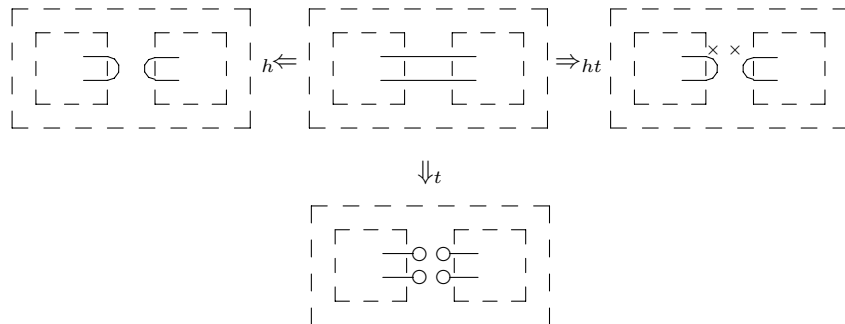
Proof: The primality and minimality conditions imply that deleting one of the segments of the pair does not change the number of connected components. The primality implies also that the segments are together in some closed string, say, a $^{+}$string. If the segments are $^{-}$open and $^{\times}$open, we have a torus of the first or second type and the down reading implication holds. Suppose that the segments are together in a closed $^{-}$string. Then they are $^{\pm}$balanced or $^{\pm}$consistent. They can not mix the balanced-consistent types because they are traversed either consistently or not for both strings.

If the pair is $^{\pm}$consistent, then the left reading implication holds as a elimination of 0, 1 or 2 handles. This follows from Theorem 10 in [FL91].

If the pair is $^\pm$balanced, and at least one segment is $^\times$open, then we can attach a pair of $^\times$charges to it and consider the segment between the charges and the other segment as a new pair, which is now $^\pm$consistent, and reduced to the previous case. However, because of the new pair of charges, the right reading implication corresponds to handle eliminations.

Finally, if both segments are $^\times$closed, then they must be on the same closed $^\times$string (because of the fact that it is separating). It follows that the the pair is *balanced for $* \in \{+, -, \times\}$. In this case the situation is of a cutting along a torus surface (of type 3) followed by the canonical closing given by the string presentation. ∎

5 A Catalogue of all Closed Orientable Prime 3-Manifolds (non-lens spaces) up to Complexity 13.

The *gem-complexity* or simply the *complexity* of a 3-manifold is defined as one less than half of the vertices of a 3-gem which represents it and has a minimum number of vertices among such 3-gems. There are finitely many 3-manifolds of a given complexity and we conjecture that this function is additive on connected sums.

In the following pages we present once each orientable closed 3-manifold up to complexity 13 (except lens spaces) [18]

The justifications for the completeness and freeness of duplicates are in [LD89] and [LD91], where the 9351 rigid 3-gems of less than 30 vertices are listed and topologically classified yielding only 44 manifolds on that class. The central details of this classification will also appear in the forthcoming book [Lin95].

From the 44 members, 38 of them are presented as interacting strings. The remaining 6 manifolds (for which we do not know a string presentation), are displayed by a 3-gem which attain the complexity (has a minimum number of vertices).

5.1 An Overview of the Catalogue and of the Listed Manifolds

In the listing of the manifolds there are 5 columns. The first one gives the complexity and the index inside a same that complexity. For instance, 11_3 means the third 3-manifold of complexity 11. The ordering among the same complexity is inherited from a slightly perturbed lexicographical order for the homology groups, see [LD89]. The next two columns are a geometrical description (whenever available) and a *symbol* for the 3-manifold. The fourth column denotes the specific 3-gem which is being presented, either in the catalogue of [LD89] or in the family $\mathcal{S}(b, l, t, c)$ [LM85]. From the diagram in the final column the manifold is recoverable.

The *symbols* we have chosen for the manifolds usually come from their fundamental groups [LS94]. QUAT is the quaternionic space, obtained by identifying opposite faces of a solid cube preceded by $\pi/2$ rotations [Mon82]. BINTET is the binary tetrahedral space, BINOCT is the binary octahedral space. (This last space is also known as the space of the truncated cube, see also [Mon82].) POINCARE$_0$ denotes the spherical dodecahedral space, the original sphere of Poincaré. There appears another $Z-$homology sphere denoted POINCARE$_1$. These are the first members of an infinite family of homology Z-spheres described as the 2-fold branched covering of S^3 over the torus knot $(3, p)$: they are cases $p = 5$ and $p = 7$.

The EUCLID family are the flat riemannian manifolds, quotients of the 3-TORUS, $\mathbf{S}^1 \times \mathbf{S}^1 \times \mathbf{S}^1$, which could be denoted as EUCLID$_0$. We observe that all the six flat manifolds are present. In particular, $\pi_1(\text{EUCLID}_1)$ is the Fibonacci group $F(2, 6) = <x_1, \ldots, x_6 \mid x_i x_{i+1} = x_{i+2}>$, subscripts mod. 6. This manifold can also be described as a 2-fold covering of S^3 branched over the alternating knot obtained from a plane drawing of the edges of an octahedron. The pEUC manifolds arise from a perturbation in the EUCLID's.

The manifold NILP(2, 2)4, which has a nilpotent quotient of its fundamental group, arises from a single Dehn-Lickorish surgery over a knot from the connected sum of 4 copies of $\mathbf{RP}^3$. It is interesting to mention that this manifold arises also from EUCLID$_3$ from the same type of operation and that these surgeries and their effect are apparent from the string presentation. There is another string presentation for $R_{24}(6)$ which does not contain ends or charges. This flat space has the smallest complexity among all manifolds with this property. It is a rare fact for connected 3-manifolds. It seems interesting to contemplate the following two manifestations of the same reality, $R_{24}(6)$:

---

[18]We consider the 3-sphere and $\mathbf{S}^1 \times \mathbf{S}^2$ as lens spaces.

The fundamental group for $<$**5,5,2**$>$**2** is a central extension of the triangle group generated by a, b, c with relators a^5, b^2, c^2, abc. If we lift [LS94] via the homology group the representing 3-gem, $G = R_{28}(202)$, (which does not have a string presentation) we get a 56-vertex 3-gem. This simplifies to a very symmetric a 30-vertex 3-gem H, realizing the triangle group, but which also does not admit a string presentation. By repeating this lifting using a permutation representation for the homology group of $|H|$ we get a second derived of G, with 150 vertices which simplifies to a 32-vertex 3-gem admitting the following delightful string presentation:
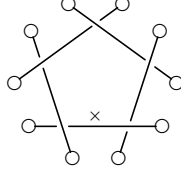
The fundamental group of the represented 3-manifold is the second derived of the fundamental group of $<$**5,5,2**$>$**2**
.

The manifolds $C^i_m C_n$ denote the elliptic 3-manifolds whose fundamental group is the semi-direct product of C_m (the cyclic group of order m) by C_n where C_n acts over C_m by inversion. Justaposition of symbols without superscripts means cartesian product. The family Q_n is the quaternion family.

There appears an interesting class of manifolds at the end of the list. The 2×2 matrix justaposed to a Z denotes the action of Z on the cartesian product $Z \times Z$.

The symbols in brackted form [ ] terminating in an S^e_g means the parameters for the derived groups, stopping at the fundamental group of a surface of genus g slightly modified in a way specified by the exponent e; these seem to be Seifert manifolds (but not quite).

For more details see the incoming article [LS94]. In the following pages follows **the catalogue.**

All Non-Trivial 3-Manifolds up to Complexity 13: $\mathbf{8_1}$ to $\mathbf{11_3}$
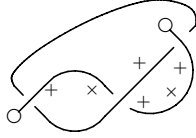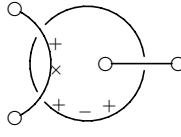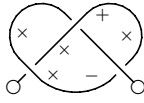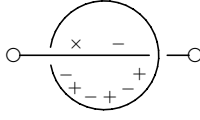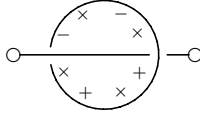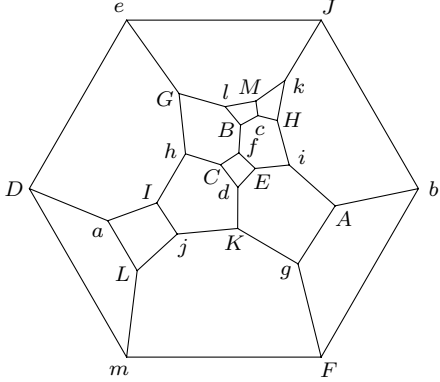
$\mathbf{8_1}$ $\mathbf{S}^3/Q_8$ QUAT $R_{18}(1):$

$\mathbf{9_1}$ $\mathbf{S}^3/(C_3^i C_4)$ $R_{20}(4):$

$\mathbf{10_1}$ $\mathbf{S}^3/P_{24}$ BINTET $R_{22}(1):$

$\mathbf{10_2}$ $\mathbf{S}^3/(C_3^i C_8)$ $R_{22}(2):$

$\mathbf{11_1}$ $\mathbf{S}^3/P_{120}$ POINCARE$_0$ $R_{28}(4079):$

$\mathbf{11_2}$ $\mathbf{S}^3/P_{48}$ BINOCT $R_{28}(4788)$

$\mathbf{11_3}$ $\mathbf{S}^3/(C_5^i C_8)$ $R_{24}(4)$

All Non-Trivial 3-Manifolds up to Complexity 13: 11_4 to 12_1

11_4 $\mathbf{S}^3/Q_{16}$ $R_{24}(154)$:
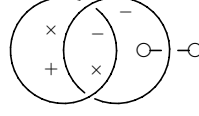
11_5 $\mathbf{S}^3/(Q_8 \times C_3)$ $R_{24}(13)$:
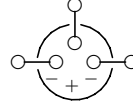
11_6 EUCLID$_1$ $R_{24}(5)$:
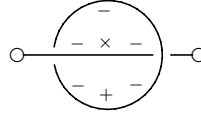
11_7 EUCLID$_2$ $R_{24}(7)$:
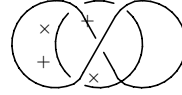
11_8 EUCLID$_3$ $R_{24}(6)$:
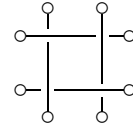
11_9 3-TORUS $R_{24}(1)$:
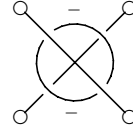
12_1 $\mathbf{S}^3/(C_7 P_{120})$ $R_{26}(10)$:
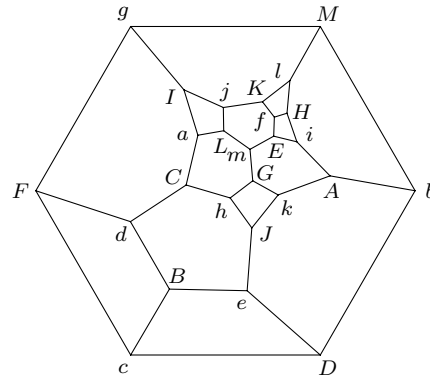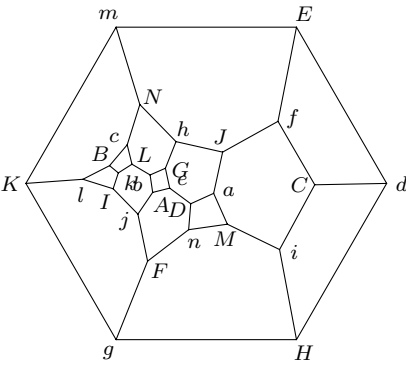
All Non-Trivial 3-Manifolds up to Complexity 13: $\mathbf{12_2}$ to $\mathbf{12_3}$
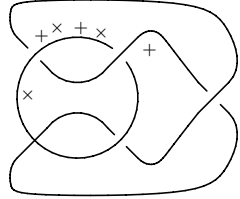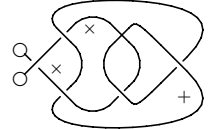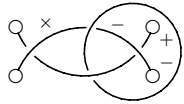
$\mathbf{12_2}$ $\mathbf{S}^3/(Q_8^N C_9)$ $R_{26}(9):$

$\mathbf{12_3}$ $\mathbf{S}^3/(C_5^i C_{12})$ $R_{26}(6):$

$\mathbf{12_4}$ $\mathbf{S}^3/(Q_8^N C_{15})$ $R_{26}(696):$

$\mathbf{12_5}$ $\mathbf{S}^3/(C_3 Q_{16})$ $R_{26}(753):$

$\mathbf{12_6}$ $\text{pEUC}_1(0,2)$ $R_{26}(5):$

$\mathbf{12_7}$ EUCLID_4 $R_{26}(31):$

All Non-Trivial 3-Manifolds up to Complexity 13: 12_8 to 13_2

12_8	EUCLID$_5$	$R_{26}(11):$	
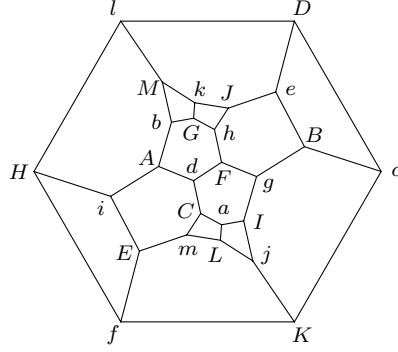
12_9	pEUC$_1(2,2)$	$R_{26}(699):$	
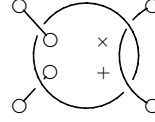
12_{10}	$Z_{-1\ 2}^{0\ 1}$	$R_{26}(695):$	
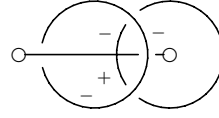
13_1	POINCARE$_1$	$\mathcal{S}(3,7,6,1):$	
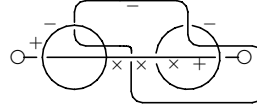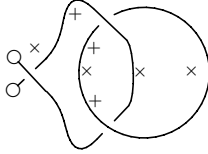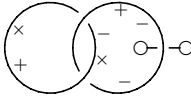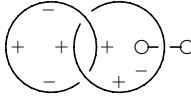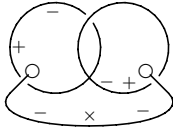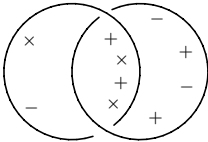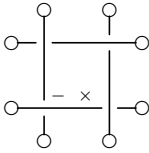
13_2	**<5,5,2>2**	$R_{28}(202):$	
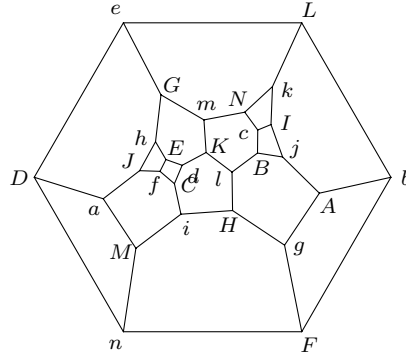
All Non-Trivial 3-Manifolds up to Complexity 13: 13_3 to 13_6

13_3 $[3, 5^2, S_6^5]$ $R_{28}(2)$:

13_4 $[3, 4^2, S_4^3]$ $R_{28}(4460)$:

13_5 $\mathbf{S}^3/(C_5^i C_4)$ $R_{28}(3882)$:

13_6 PSL(2,3,7)5 $R_{28}(203)$:

All Non-Trivial 3-Manifolds up to Complexity 13: $\mathbf{13_7}$ to $\mathbf{13_{11}}$

$\mathbf{13_7}$ $\mathbf{S}^3/(C_7^i C_8)$ $R_{28}(2314):$
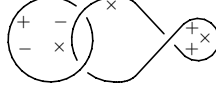
$\mathbf{13_8}$ $\mathbf{S}^3/(C_7^i C_{12})$ $R_{28}(4510):$
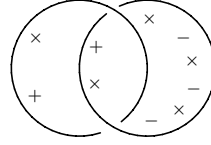
$\mathbf{13_9}$ $\mathbf{S}^3/(C_3^i C_{16})$ $R_{28}(27):$
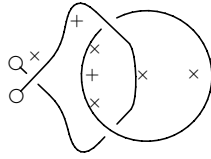
$\mathbf{13_{10}}$ $\mathbf{S}^3/(C_3^i C_{20})$ $R_{28}(29):$
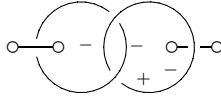
$\mathbf{13_{11}}$ $[24, S_2^1]$ $R_{28}(1):$
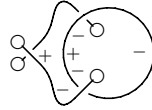
All Non-Trivial 3-Manifolds up to Complexity 13: 13_{12} to 13_{17}

13_{12} $[2^2, 3^2 \times 6, S_5^9]$ $R_{28}(3)$:

13_{13} $\mathbf{S}^3/(C_3 Q_{32})$ $R_{28}(56)$:

13_{14} $\mathbf{S}^3/(C_5 Q_8)$ $R_{28}(7)$:

13_{15} $[3^2, S_1^3]$ $R_{28}(34)$:

13_{16} $\text{pEUC}_1(0, 4)$ $R_{28}(19)$:

13_{17} $\text{NILP}(2, 2)4$ $R_{28}(6)$:

All Non-Trivial 3-Manifolds up to Complexity 13: 13_{18} to 13_{21}

13_{18} $Z^{0\ 1}_{-1\ 3}$ $R_{28}(5)$:

13_{19} $Z^{0\ 1}_{-1\text{-}3}$ $R_{28}(4557)$:

13_{20} $Z^{1\ 0}_{2\ 1}$ $R_{28}(42)$:

13_{21} $Z^{1\text{-}2}_{0\ 1}$ $R_{28}(4466)$:

References

[BZ84]   M. Boileau and H. Zieschang. Heegaard genus of closed orientable Seifert manifolds. *Invent. Math.*, 76:455–468, 1984.

[Fer87]   M. Ferri. Colour switching and homeomorphisms of manifolds. *Canadian J. Math.*, 39:8–32, 1987.

[FG82]   M. Ferri and C. Gagliardi. Crystallization moves. *Pacific J. Math.*, 100:85–103, 1982.

[FL91]   M. Ferri and S. Lins. Topological aspects of edge fusions in 4-graphs. *J. Combin. Th. (B)*, 51:227–243, 1991.

[Gag79]   C. Gagliardi. A combinatorial characterization of 3-manifold crystalizations. *Boll. Un. Mat. Ital.*, 16-A:441–449, 1979.

[Jor79]   K. Jorhannsen. On homotopy equivalence of 3-manifolds with boundary. In *Lecture Notes in Mathemnatics, 736*. Springer Verlag, 1979.

[JS79]   W. Jaco and P. B. Shalen. Seifert fibered spaces in 3-manifolds. In Amer. Math. Soc., editor, *Amer. Math, Soc. Memoirs*, volume 220, 1979.

[Kir78]   R. Kirby. A calculus for framed links in S^3. *Inv. Math.*, 45:35–56, 1978.

[LD89]   S. Lins and C. Durand. A complete catalogue of rigid graph-encoded orientable 3-manifolds up to 28 vertices. *Notas Com. Mat. UFPE*, 168, 1989.

[LD91]   S. Lins and C. Durand. Topological classification of small graph-encoded orientable 3-manifolds. *Notas Com. Mat. UFPE*, 177, 1991.

[Lic62]   W. B. R. Lickorish.   A representation of oriented combinatorial 3-manifolds.   *Annals of Mathematics*, 76:531–540, 1962.

[Lin85]   S. Lins. A simple proof of Gagliardi's handle recognition theorem. *Discrete Math.*, 57:253–260, 1985.

[Lin88]   S. Lins. On the fundamental group of 3-gems and a "planar" class of 3–manifolds. *Europ. J. Combinatorics*, 9:291–305, 1988.

[Lin89]   S. Lins. Um cálculo diagramático para variedades tridimensionais. Thesis presented at UFPE, 1989.

[Lin92]   S. Lins. A 3-gem construction for the closed orientable 3-manifolds. *Submitted*, 1992.

[Lin95]   S. Lins. Gems, Computers and Attractors for 3-Manifolds. In *to be published in the series Knots and Everything*. World Scientific, 1995.

[LM85]   S. Lins and A. Mandel. Graph-encoded 3-manifolds. *Disc. Math.*, 57:261–284, 1985.

[LS94]   S. Lins and S. Sidki. The fundamental groups of 3-manifolds triangulizable by less than 30 tetrahedra each 4 vertex-colored. *To appear in the Int. J. Alg. Comput.*, 1994.

[Mat91]   S. V. Matveev. Complexity theory of three-dimensional manifolds. *Acta AplicandæMathematicæ, to appear*, 1991.

[Mon82]   J. Montesinos.   Variedades de mosaicos.   Sexta Escuela Latinaamericana de Matematicas, Oaxtepec - Mexico, 1982.

[Mon89]   J. Montesinos. La discrepancia entre el rango y el genero de heegaard de una 3-variedad. *Note di Matematica*, 9:101–117, 1989.

[Mos73]   G. D. Mostow. Annals of mathematical studies. In *Strong rigidity of locally symmetry spaces*, volume 78. Princeton University Press, 1973.

[Rol76]   D. Rolfsen. *Knots and links*. Publish or Perish, 1976.

[RT76]   F. Raymond and J. L. Tollefson. Closed 3-manifolds with no periodic maps. *Trans. A.M.S.*, 221:401–418, 1976.

[Wal60]   A. H. Wallace. Modifications and cobounding manifolds. *Can. J. Math.*, 12:503–528, 1960.